The importance of 3D fibre architecture in cancer and implications for biomaterial model design

J.C. Ashworth[1,2,3*] & T.R. Cox[3,4*]

[1]School of Veterinary Medicine & Science, Sutton Bonington Campus, University of Nottingham, Leicestershire, LE12 5RD, UK; [2]Biodiscovery Institute, School of Medicine, University of Nottingham, Nottingham, NG7 2UH, UK; [3]Cancer Ecosystems Program, The Garvan Institute of Medical Research and The Kinghorn Cancer Centre, Darlinghurst, NSW, Australia; [4]School of Clinical Medicine, St Vincent's Healthcare Clinical Campus, UNSW Medicine and Health, UNSW Sydney, Sydney, NSW, Australia

*Correspondence to Jennifer.Ashworth@nottingham.ac.uk and t.cox@garvan.org.au

This version of the article has been accepted for publication, after peer review, but is not the Version of Record and does not reflect post-acceptance improvements, or any corrections. The Version of Record is available online at: http://dx.doi.org/10.1038/s41568-024-00704-8

Abstract

The need for improved prediction of clinical response is driving the development of cancer models with enhanced physiological relevance. A new concept of 'precision biomaterials' is emerging, encompassing patient-mimetic biomaterial models that seek to accurately detect, treat, and model cancer, by faithfully recapitulating key microenvironmental characteristics. Although recent advances allow tissue-mimetic stiffness and molecular composition to be replicated *in vitro*, approaches for reproducing the 3D fibre architectures found in tumour extracellular matrix (ECM) remains relatively unexplored. Whilst the precise influences of patient-specific fibre architecture are unclear, we summarise the known roles of tumour fibre architecture, underlining their implications in cell-matrix interactions and ultimately clinical outcome. We then explore the challenges in reproducing tissue-specific 3D fibre architecture(s) *in vitro*, highlighting relevant biomaterial fabrication techniques and their benefits and limitations. Finally, we discuss imaging and image analysis techniques (focussing on collagen I optimised approaches) that could hold the key to mapping tumour-specific ECM into high fidelity biomaterial models. We anticipate that an interdisciplinary approach, combining materials science, cancer research and image analysis, will elucidate the role of 3D fibre architecture in tumour development, leading to the next generation of patient-mimetic models for mechanistic studies and drug discovery.

[H1] Introduction

The cells in our bodies are surrounded by an intricate network of fibrillar **[G]** and non-fibrillar proteins, glycoproteins, and polysaccharides. This network, termed the extracellular matrix (ECM), is known to play vital roles in disease progression, influencing many of the biological processes underpinning the hallmarks of cancer[1,2]. ECM composition, structure and mechanical properties all have critical influences on cell behaviour, varying according to tissue and disease state[3–5]. As such, there is an increasing focus on harnessing *in vitro* and *in vivo* disease models to replicate and study these tissue-specific relationships. While cells cultured in 2D can lack appropriate cell polarity, phenotype and tissue organisation[6,7], 3D culture systems are being increasingly adopted due to their ability to reflect a more physiologically relevant environment[8,9]. In recent years, there has been particular focus on the development of biomaterials for recreating tissue-realistic ECM microenvironments: a topic known as 'precision biomaterials'[10–13].

Given the notoriously high attrition rate in current drug discovery pipelines[14], advanced 3D models could act as more predictive preclinical models of patient response[15]. For this to be achievable, it is crucial to ensure that these 3D models can accurately capture real-life disease progression mechanisms and tissue-specific cell phenotypes. This would have the potential to improve the identification of targetable mechanisms specific to cell-matrix interactions. Recent analysis has shown that most current cancer therapies target mechanisms independent of the surrounding microenvironment[16], indicating huge untapped potential for new, undiscovered therapies targeting the role of the ECM.

While there is now a large body of research focussed on the design of biomaterials with tissue-realistic stiffness and, more recently, controlled composition[17–19], reproducing the complex 3D fibrous architectures found in the cancer stroma within a high-fidelity scalable biomaterial model is still an unmet challenge. While models with controlled composition generally focus on altering the relative proportions of individual, or small numbers of ECM constituents[20], their potential to replicate specific fibre **[G]** patterns, orientations and feature sizes found in native tissue remains relatively unexplored. This has, in part, been hindered by the vast heterogeneity of ECM architecture found in tumours. This Review addresses this knowledge gap, highlighting the need for such tissue-realistic biomaterial models of fibre architecture, discussing the challenges involved in their design and fabrication, and outlining the current state-of-the-art technologies used in reproducing tissue-specific 3D fibre networks *in vitro*. We highlight the need for a multidisciplinary approach in designing the next generation of precision tissue models, combining new innovations in materials science with advanced microscopy and image analysis techniques (Fig. 1). In the context of this review, we define 'fibre' as any elongated structural unit within biomaterials or in tissue, including those composed of ECM proteins and synthetic substances.

[H1] Role of 3D fibre architecture in cancer

[H2] Changes in ECM architecture during tumorigenesis

The ECM may broadly be divided into two components: the interstitial ECM **[G]** and the basement membrane **[G]**. In normal, non-diseased tissue, the ECM undergoes constant remodelling, but this process becomes dysregulated in cancer, leading to changes in both ECM deposition and degradation[21]. Remodelling of both the interstitial matrix and the basement membrane is observed in cancer, with for example, a loss of the basement membrane disrupting apicobasal polarity and bringing epithelial cells into contact with the interstitial matrix[3].

ECM remodelling in cancer is a complex process, involving crosstalk between the heterogeneous cell populations within the tumour microenvironment. For instance, growth factors secreted by cancer cells and immune cells play a role in fibroblast recruitment and activation to cancer associated fibroblasts (CAFs)[22]. Transforming growth factor β (TGFβ) signalling is perhaps the most well-known mechanism of fibroblast activation to CAFs, but there are many other examples, including increased tissue stiffness and DNA damage, for example from chemotherapy[23]. This indicates positive feedback loops by which tumour-associated ECM remodelling likely helps sustain the CAF phenotype, instead of the deactivation that would be seen in normal wound repair and tissue remodelling[24]. Although CAFs are the main drivers of tumour remodelling, being the main producers of ECM in the interstitial matrix, tumour cells can also contribute to ECM synthesis[5,25–30]. Other remodelling processes also include regulation by the release of proteases (including matrix metalloproteinases (MMPs) and cathepsins); post-translational modifications, such as glycosylation, sulfation, and cross-linking *via* enzymes (including lysyl oxidases (LOX) and transglutaminases); and force-mediated remodelling *via* integrins[22,23,31–35]. The combination of these processes leads to the development of discrete, often highly heterogenous (both spatially and temporally) tumour tissue-specific ECM. This tumour-specific ECM is typically of higher stiffnesses relative to associated normal tissue, as well as altered ECM composition, whereby the amount, and the types of ECM molecules secreted differ from that of the normal tissue[27]. Together, these changes directly influence progression and metastatic potential[5,32,36].

Moreover, these changes are accompanied by reorganisation of the 3D fibre network in the interstitial matrix, which is thought to be highly dependent on cell contractility[37,38]. Typically, randomly oriented fibres are indicative of normal stroma, whereas aligned and often thickened fibres are indicative of tissue fibrosis and tumour development[39]. However, this is highly dependent on tumour type. Breast and pancreatic cancers are often considered examples of highly fibrotic tumours, due to the relatively high density of matrix deposition compared with other tumours[40]. Heterogeneity in ECM microarchitecture is also apparent even within a single tumour type, for instance in colorectal cancer high variability has been observed between patients, but with an overall trend of increasing collagen alignment in colon carcinoma compared to normal tissue[41]. A range of collagen fibre morphologies can also be observed in human breast cancer patient tissue, ranging from wavy to straight, thick to thin, and high to low density[42].

[H2] Clinical significance of 3D architecture

Much of the earliest pioneering work examining the link between fibre organisation and patient prognosis focussed initially on breast cancer. It has long been recognised that mammographic density, which is associated with an increase in stromal matrix proteins, is one of the strongest independent risk factors associated with breast cancer onset[43,44]. More recently, tissue from regions of high mammographic density has been found to correlate with increased prevalence of long, aligned bundles of fibrillar collagen, rather than with levels of amorphous collagen **[G]**[45]. In a seminal study, biopsied tissue sections from human breast carcinoma were imaged using second harmonic generation microscopy and categorised according to the presence and alignment of collagen fibres at the tumour boundary, defining a set of tumour-associated collagen signatures (TACS)[46]. In a mouse model of breast cancer, increasing TACS level from TACS-1 to TACS-3, representing transition from early stage to late stage tumourigenesis, corresponded to an increase in directional local cell invasion. In clinical samples, TACS-3 score is also an independent prognostic factor related to poor disease-specific and disease-free survival (Fig. 2A)[47]. Building on this concept, recent work indicates that tumours have highly heterogeneous structures on larger length scales. Whether the intra-tumour heterogeneity of collagen fibre architecture, both in and around the tumour, is driven by the cellular heterogeneity known to be present in tumours, or itself contributes to establishing that cellular

heterogeneity remains unknown. That said, the prognostic value of the TACS score may be improved by considering additional categories of collagen structure further from the tumour boundary[48].

Features resembling TACS-specific fibre organisation can also be observed in other tumours, including pancreatic ductal adenocarcinoma (PDAC). Here, TACS-3 like structures representing conduits for invasion are present both in early preinvasive cancer (defined histologically), and in more advanced disease[49]. Combined with evidence of early-stage cancer cell dissemination in the KPC mouse model, this suggests that TACS scores may discriminate disease progression to a greater extent than is possible using standard histology. Further aspects of 3D collagen arrangement are found to vary with disease progression in other tumour types but are less clearly categorised. For instance, in ovarian cancer, collagen fibres become more crimped than in normal tissue (Fig. 2C), but the overall changes in collagen alignment are less clear-cut and highly heterogeneous both between and within patients[50,51]. The effect of collagen fibre alignment is also complex in basal cell carcinoma (BCC), with increased alignment in BCC samples compared with normal tissue and benign lesions. Paradoxically, highly aligned bundles were associated with the least aggressive BCC subtypes, measured relative to other collagen fibres rather than to the tumour boundary in contrast to the TACS scores discussed previously[52]. Importantly, this study highlighted that parallel organisation of collagen bundles was still a more effective marker for BCC than the parameters of individual collagen fibres (i.e. width, length, angle, and straightness). Fibre characteristics beyond density and alignment also have clinical relevance in many settings: for instance, increased thickness of periductal collagen fibres has been linked to low survival in PDAC patients (Fig. 2B)[53]. Another recent study identified increased fibre "straightness" as a potential diagnostic marker indicating the presence of non-small cell lung cancer[54]. Interestingly, high fibre width and low fibre alignment were also associated with poor survival, but only in lung adenocarcinoma, highlighting the need for disease-specific consideration of the role of different fibre architecture(s) (Fig. 2F).

Notably, the impact of ECM fibre architecture and ECM remodelling is not restricted to the primary tumour but is also observed in metastasis. For instance, fibrosis of metastatic lymph nodes in colorectal cancer has been shown to correlate with lower survival[55]. Collagen fibre orientation in ovarian cancer metastases has also shown strong correlation with disease score and outcome[56]. Interestingly, relative collagen abundance was decreased in diseased tissue, due to the increased levels of other proteins such as fibrinogen and fibronectin. Secretion of other matrix molecules such as fibronectin in a fibrotic, collagen-rich lung has been shown to chemoattract hepatoma and breast carcinoma cells in a mouse model of metastasis[57]. Regions of fibronectin accumulation have also been suggested to bind various LOX, proteins enhancing fibrillar collagen crosslinking and bundling, contributing to the formation of a pre-metastatic niche[58]. Supporting this finding, LOX activity was responsible for developing a collagen-rich, fibrotic microenvironment permissive to breast cancer metastasis in mouse models of pulmonary fibrosis[59].

3D fibre architecture is also known to change during chemotherapeutic, radiotherapeutic and targeted therapy treatment. These therapies can induce tissue fibrosis through the generation of reactive oxygen species, DNA damage, rewiring of intracellular signalling, and inflammation[31,60–63]. This therapy-induced fibrosis likely plays an important role in recurrence and metastasis, as well as the debilitating side-effects of therapy, as reviewed elsewhere[64,65]. In a study of matrix-mediated drug resistance in melanoma, BRAF inhibition was seen to increase collagen fibre area and thickness, through clustering of phosphorylated discoidin domain receptors (DDRs) along collagen fibres[66]. Interestingly, the hormonal therapy tamoxifen, has also been reported to decrease mammographic density, when given as a preventative strategy to patients at high risk of breast cancer[67].

While most of the above discussion focusses on the tumour-promoting role of tissue fibrosis, some studies also indicate a tumour-suppressive role of increased matrix density. Using a mouse model of pancreatic cancer, one study found that some highly aggressive tumours induced by sonic hedgehog deficiency had reduced stromal content and increased vascularity[68]. In rats, investigations into pregnancy-associated changes in collagen density revealed an increase in fibrillar collagen correlating with decreased tumour incidence[69]. These matrices had more randomly aligned collagen fibres, and lower overall stiffness, suggesting multiple factors related to 3D fibre architecture may be at play. Similar increases in collagen I were observed in samples from premenopausal parous women relative to nulliparous women. It has also been suggested that the role of fibrotic tissue in tumour growth or suppression is dependent on the stage of tumour development[70]. It is, however, clear that the clinical implications of fibre arrangement at both the primary and metastatic sites are extensive, tumour-specific, and highly heterogeneous.

[H2] Role in cell-matrix interactions

[H3] Cell adhesion and migration

Changes in ECM microarchitecture subsequently alter the arrangement (and presentation) of adhesion sites, which can directly impact bidirectional cell-matrix interactions, thereby affecting cellular behaviour and ultimately tissue function and/or disease progression[71]. Cell-matrix adhesion sites provide an interactive interface between the extracellular chemical and physical milieu, and intracellular scaffolding and signalling networks. This dynamic, reciprocal regulation is predominantly orchestrated by membrane receptors known as integrins[72]. When the cell pulls or pushes on the matrix, mechanical signals are transformed into biochemical responses in a process known as mechanotransduction (discussed in further detail below). This can trigger cell migration, proliferation, differentiation and intracellular signaling[73].

The specific pore size within a matrix is also known to be crucial for regulating cell motility[74–76]. In an ECM structure with pore sizes above the nuclear diameter, cell migration can occur without proteolysis by exploiting existing microtracks in the ECM network. The mode of migration used in this case is dependent on cellular properties including contractility and adhesion to the matrix[77]. For instance, at pore sizes above 2.5 µm diameter, HT1080 fibrosarcoma cells migrate by deforming their nuclei, upregulating integrin activation and cell contractility[78,79]. At lower pore sizes, MMPs become necessary for migration, and evidence suggests that the exact pore size level of this transition is cell type dependent.

Fibrillar wave amplitude has also been shown to affect directional cancer cell migration. Over a certain amplitude, wavy fibrillar networks can act as a barrier to cell polarisation, with the exact level depending on the myosin contractility of the migrating cells[80]. Such ECM barriers to migration can secondarily impact cancer cell metabolism. In particular, the ATP:ADP ratio is impacted by collagen density and fibre alignment. Specifically, the ATP:ADP ratio increases in cells in denser matrices, where migration is impaired and decreases in cells in aligned collagen matrices, where migration is facilitated. This is thought to relate to the energy required for cancer cells to remodel and migrate through the matrix[81]. Moreover, integrin switching **[G]** can occur as the biochemistry and microarchitecture of the tumour matrix evolves[82,83]. Such changes are thought to influence how tumour cells navigate the heterogenous 3D tissue, and importantly, how they are stimulated to transition between modes of invasion such as mesenchymal, amoeboid and collective invasion **[G]**[84,85].

[H3] Collective cell invasion

The switch between single cell and collective invasion has been shown to relate to collagen density, *via* cell jamming **[G]** in high density matrices[86]. Intravital imaging of collective cell invasion in an *in vivo* B16F10 mouse model of melanoma demonstrated that leader cells preferentially exploit existing ECM channels to invade, rather than generating new paths[87]. Supporting this work, collectively invading cells following microtracks **[G]** in the collagen fibre network have also been observed in tissue sections from human breast carcinoma[88], and prior work demonstrated that both collective invasion and collagen alignment correlate with metastatic outcome in patients with breast cancer[46,47,89,90]. Collective cell invasion in squamous cell carcinoma (SCC) may be promoted by fibroblast-mediated matrix remodelling, and deposition of fibronectin and tenascin-C, to create physical tracks for cancer cell migration[91]. Similar patterns were observed in organotypic *in vitro* assays (collagen I and Matrigel) and in clinical samples from SCC patients (Fig. 2D).

[H3] Immune response

While the immune response and its relationship to the ECM in cancer is a very broad research area and has been reviewed elsewhere,[92,93] here we highlight a few key studies relating to fibre architecture. One study has shown that matrices of high collagen density compared to lower, decreased T cell proliferation, increased $CD4^+$ T cell to $CD8^+$ T cell ratio, and reduced T cell cytotoxic activity[94]. Another study, using viable slices of patient-derived lung tumours, found that immune cell infiltration correlated with increased fibre orientation and decreased collagen and fibronectin density within the tumour stroma[95]. Similarly, a study examining BCC histological sections found correlations between matrix organisation and the number of tumour infiltrating lymphocytes (TILs), where increasing fibre length and lacunarity, or decreasing matrix density increased the number of TILs (Fig. 2E)[96].

[H3] Paracrine interactions

ECM organisation also influences molecular transport through tumour tissue, and alters the cancer cell secretome[97,98]. Hormone-restricted breast tumour cells cultured on aligned matrices show a modified secretome that increases tumour cell proliferation relative to randomly aligned matrices[98]. High matrix density and alignment can also alter molecular transport by confining molecular diffusion to the direction of fibre alignment, which could alter inter-cellular transport of signalling molecules[99]. *In silico* computational studies, modelling the predicted effect of matrix remodelling at a tumour-stroma interface, have also found an increase in circumferential, relative to radial, permeability at the tumour boundary, likely due to the circumferential orientation of collagen fibres, although this has yet to be confirmed in *in vitro* or *in vivo* models[100]. Interestingly, the arrangement of ECM fibres affects the formation of tunnelling nanotubes (TNTs) **[G]**, such that when mesothelioma cells were cultured on aligned matrices, the cells formed longer, but fewer TNTs relative to cells on cross-hatched matrices[101]. Given the proposed role of TNTs in regulating cell-cell interactions[102], these matrix effects on TNTs may alter long-range cell-cell communication[101].

[H3] Mechanotransduction

Changes in matrix microarchitecture can also alter how forces propagate through and deform tissues[103]. Alterations in microarchitecture can both enhance and diminish viscoelastic behaviour, influencing tissue and cellular response to mechanical stress[104]. Computational simulations have suggested that cells in a fibrous matrix can sense long-distance mechanical cues, from distances up to 20 times their diameter[105]. Fibre architecture has also been shown to regulate the trans-differentiation of adipose stromal cells into myofibroblasts, with an increase in cell contractility and α-smooth muscle

actin (αSMA) staining observed in cells in matrices with thick fibres and large pores[106]. Moreover, higher TACS scores correlate with ephrin type-A receptor 2 (EPHA2) non-canonical signalling, which is thought to be involved in TWIST1-mediated activation of epithelial-to-mesenchymal transition (EMT) in *in vitro* and *in vivo* models of breast cancer[107]. Interestingly, mechanotransduction has also been linked to mechanisms of chemoresistance in breast cancer cells cultured on aligned nanotopographies, *via* upregulation of aryl hydrocarbon receptor (AhR) and cytochrome p450 family 1 (CYP1) signalling to protect against chemotherapy-induced oxidative stress[108].

[H1] Biomaterial-based approaches for controlling 3D fibre architecture

Whilst the many different polymeric biomaterials used in cancer research have been extensively discussed previously[109], here we focus on how biomaterial models may be developed and applied to study mechanisms of cancer progression relating to tissue-specific 3D fibre architecture (Fig. 1B, Fig. 3). Since much is still unknown as to how specific matrix microarchitecture alters tumour progression, a reductionist approach is typically taken, whereby careful and robust mimicking of a small number of matrix parameters is prioritised over recapitulating the complexity observed in tumours (Fig. 1A). However, we must note that there exists a fine balance between reductionist approaches aimed at asking defined questions, and accurately recapitulating the complexity.

[H2] Hydrogels

Hydrogels are defined as networks of hydrophilic polymers with characteristically high water content[110,111] (Figure 3). Typically sub-categorised as naturally-derived or synthetic hydrogels (Fig. 3), arguably the most well-known example is Matrigel, a naturally-derived hydrogel with well-established applications for tumour growth, invasion and angiogenesis assays, and more recently the establishment of 'living biobanks' of patient-derived organoids[112,113]. Matrigel is one of several commercially available hydrogel products derived from Engelbreth-Holm-Swarm (EHS) mouse tumours and referred to as basement membrane extracts. However, since the animal-derived nature of Matrigel results in batch-to-batch variation and poorly defined composition, there has been a recent push for more well-defined alternatives[114].

Naturally-derived hydrogels can also include collagen, alginates, gelatin and hyaluronic acid[115–117]. In some cases, synthetic components or functional groups are incorporated for crosslinking, in which case the hydrogel may be considered a 'hybrid material'[110]. Equally, hydrogels fabricated using primarily synthetic materials have important applications in cancer research. In particular, pioneering work has demonstrated the application of poly(ethylene glycol) (PEG) as an alternative to Matrigel for the successful expansion of mouse and human-derived intestinal organoids[18]. These PEG-based gels may be functionalised by the addition of full-length ECM proteins, glycans or ECM-mimetic peptide sequences, further increasing the versatility of the system. Similarly, synthetic hydrogels fabricated from self-assembling peptides can be modified using full-length ECM proteins and glycans[17].

Application of hydrogels for 3D cancer modelling is a popular approach, given their ability to mimic key features of the tumour microenvironment[118]. This includes the ability to control mechanical properties such as stiffness and viscoelasticity[119,120], within a physiologically relevant range, as reviewed elsewhere[121]. Synthetic systems can, in some cases, provide superior control over mechanical properties compared with naturally-derived matrices, particularly in the case of PEG gels, which may also be designed to be mechanically dynamic[122,123]. Such synthetic systems also avoid the reproducibility issues commonly seen in naturally-derived hydrogels[123], and enable the relatively cost-effective incorporation of bioactive ligands[124]. Arguably, however, native ECM accounts for the

possibility of multiple binding sites on a single protein, as well as for the alternative ECM isoforms that may be seen in cancerous tissues, such as those resulting from splice variants[125].

[H3] Control of 3D fibre organisation in hydrogel-based materials

While the versatility of hydrogels in mimicking tissue-realistic stiffness and composition is well-established, it has recently been recognised that such systems do not typically mimic *in vivo* fibre architecture[126,127]. As such, techniques for patterning fibre networks in hydrogels are becoming more established, including methods of controlling pH and temperature of gelation[83,106,135,136], as well as inducing directionality with laminar or Marangoni flow[128,129], chemical gradients[130], magnetic fields[131], and/or electric fields[132,133].

For example, one key study used pH and collagen concentration to control the rate of collagen fibrillogenesis, producing independent changes in pore size and fibril diameter[134]. This was a powerful tool for elucidating the roles of different 3D fibre architectures on cell behaviour, revealing that increasing collagen fibril diameter promotes both mesenchymal and amoeboid cell invasion, independent of matrix stiffness and pore size. In another study, a similar effect was achieved by varying the temperature of collagen gelation, with lower gelation temperatures giving longer and thicker collagen fibres[135]. These thicker fibres were observed to increase vascularisation and anastomosis **[G]** of endothelial cells cultured in collagen gels supplemented with Matrigel. As this effect was abrogated upon IL-8 inhibition, the authors hypothesised that the thicker fibres induced vascularisation through IL-8 secretion altering integrin engagement. Adding sodium sulphate during the gelation process, a salt with strong collagen binding affinity, also induced bundling of collagen fibrils into thicker fibres, which decreased the velocity of invading HeLa cells[136].

Fibre organisation and orientation may also be induced in hydrogels by the application of mechanical forces during or after fibrillogenesis, which generates alignment along the direction of the induced mechanical strain[137,138]. A typical approach for this is to stretch collagen gels between two pins, producing alignment that increases with increasing strain[137,139]. One study used this approach to demonstrate that migration persistence, but not speed, was increased in matrices with higher collagen alignment[137]. Mechanical agitation during gelation has also been observed to influence the characteristics of the resulting fibre network[140,141]. Disrupting the gelation process in this way created long, thick and entangled fibres more closely mimicking those seen in fibrotic tissues, and enhanced invasion of cancerous MDA MB 231 and non-cancerous MCF10A breast epithelial cells compared to a standard collagen gel[140]. Another simple, yet elegant, approach uses warm water in collagen gel precursor to disrupt hydrogel formation[141]. This technique creates thick collagen bundles reminiscent of the early stages of breast cancer, specifically the TACS-2 morphology (Fig. 2A). These bundles can then be re-organised post-production using flow alignment or incorporated into a composite system by embedding them into agarose gels of differing concentrations.

Highly aligned hierarchical structures can also be induced through exploiting the tensile stress generated when dilute hydrogels dry in confined conditions. This method has been used to align polymer hydrogels such as alginate and cellulose, noting that the polymer backbone must be rigid enough to allow reorientation (not deformation) along the direction of mechanical stress[126]. To our knowledge, this has not yet been applied for 3D cell culture. Another study used a force-guided method to induce collagen fibre alignment, using shear forces generated by coaxial rotating cylinders during fibre nucleation, followed by gravity-induced fibre elongation[138]. Interestingly, although tumour spheroids could be incorporated into this system, their presence interfered with fibre elongation, leading to different fibre orientations on either side of the spheroids. Nonetheless, this enabled the study of the role of fibre directionality on the characteristics of breast cancer invasion.

[H3] Limitations and future directions

Unfortunately, the range of fibre diameters achievable in hydrogel-based systems is relatively low, generally from the nanometre scale up to 1 µm[127,142,143], although more recent innovations in hydrogel technology increase this range up to 10 µm[141,144]. This is still, however, lower than the largest fibre diameters found in cancer tissue, which may reach 25 µm or above[53]. Moreover, many methods for altering fibre organisation also intrinsically alter the density and/or stiffness of the matrix, complicating the biological read-outs of the effect of each parameter individually[94,127,145]. In a recent study that incorporated cellulose nanocrystals (CNCs) into gelatin hydrogels to control pore size, mechanical stiffness and fibre thickness, these parameters could only be varied concurrently. Increasing CNC concentration led to a combined decrease in pore size, increase in stiffness and decrease in fibre diameter, albeit whilst retaining a constant level of cell-adhesive ligands[127]. Independently varying key hydrogel properties such as these, both in time and space, is of much interest for advanced hydrogel-based cancer models.

We and others have also shown that interpenetrating networks (IPNs) may be used to decouple the influences of stiffness and collagen fibre density. IPNs used for this purpose combine collagen with a second hydrogel, usually one that lacks bioactive ligands, although can be applied to mixtures of collagen and Matrigel. In this way, collagen density may be controlled while simultaneously tuning hydrogel stiffness, for example by varying the degree of methacrylation in gelatin methacrylate (GelMA) hydrogels or the concentration of peptide in self-assembling peptide hydrogels[122,146]. Independent variation of collagen concentration in this manner has demonstrated the influence of collagen fibre density on cell alignment, proliferation and angiogenic potential[17,122,146]. For example, the use of collagen-GelMA IPNs demonstrated that MDA MB 231 breast cancer cells require a fibrous collagen microarchitecture for efficient invasion, while endothelial cells do not[146].

Another potential solution to this problem is through deploying macromolecular crowding. This uses macromolecules such as PEG to alter polymerisation and fibril formation in hydrogels such as collagen I. It increases the nucleation rate, and therefore fibre density, by increasing local concentration of collagen molecules, while keeping the overall collagen concentration constant[142]. Importantly, this method has recently been adapted to allow control over fibre architecture while maintaining a constant mechanical stiffness[147]. Application of 8 kDa PEG as a molecular crowding agent could control both pore size and fibre length in 2.5mg/ml collagen matrices, with no significant changes in stiffness. This induced a change from single cell to collective migration when MDA-MB-231 cells were cultured in matrices with macromolecular crowding, likely due to the smaller pore sizes and shorter fibre lengths[148]. Extension of these findings will be necessary to further delineate the roles of each fibre parameter in cancer.

[H2] Fibrous scaffolds

Fibrous scaffolds are a subtly different class of biomaterials to hydrogels, generally created by fibre-by-fibre deposition rather than the process of self-assembly and cross-linking involved in hydrogel gelation. Electrospinning, one of the most common methods for creating fibrous scaffolds, uses electrostatic forces to generate fibres (Fig. 3B). Using this technique, fibre diameter may be controlled between 3 nm and 1 mm[149]. This is a much greater range than is typically achievable by self-assembly, which typically produces fibre diameters up to ~10 µm[141,144]. Although more commonly applied in the tissue engineering field, electrospun scaffolds have been investigated for their potential in cancer modelling applications. Using electrospun polycaprolactone (PCL) scaffolds to culture Ewing sarcoma cells has demonstrated comparable gene expression and chemotherapeutic response to that observed *in vivo*, unlike 2D monolayer culture[150].

[H3] Control of fibre-by-fibre deposition

Electrospinning is a common technique for fabricating fibrous scaffolds, allowing substantial control over the properties of the fibre network. Broadly, this technique creates fibres by driving a polymer solution through a needle using a syringe pump in the presence of an electric field. Fibres are then deposited onto a collector plate, which if static, results in a random fibre network, or if rotated, can result in an aligned network[151]. Such an aligned fibre network was shown to upregulate markers related to EMT in cells isolated from the MMTV-Her2/neu transgenic mouse model of breast cancer[152]. Other parameters of the electrospinning process, including flow rate, polymer concentration and electric field strength, can be varied to control fibre diameter, pore size and porosity, as previously reviewed[151]. Although such properties are often interdependent, further control may be gained by integrating other techniques, such as the use of porogens[153]. These techniques are of particular interest in the tissue engineering field as they typically enhance cell infiltration into the scaffold[154].

'FiberGel' is an alternative technology allowing independent control over fibre diameter, stiffness and orientation[155]. By sequentially stretching and folding a core-shell structure of gelatin surrounded by PCL, fibre diameter may be controlled within a range of 500 nm – 100 µm, while also determining pore and channel width. The number of folds determines the final fibre diameter, and subsequent photo-crosslinking of the gelatin enables independent control over stiffness. Unlike many techniques for creating fibrous scaffolds, this readily allows cell encapsulation within the fibre network, prior to cross-linking the final structure with light[155]. Another approach is counter-rotating extrusion **[G]**, where a high concentration (4-5% by weight) of gel or insoluble collagen is extruded through a system of two rotating cones[156,157]. This produces a collagen film made up of 2-4 µm thick fibres, and since the rotation speeds of the extrusion cones can control collagen fibre orientation across the film cross-section, the approach can generate fibre orientation gradients[157].

[H3] Limitations and future directions

Many methods for fabricating fibrous scaffolds are incompatible with cell viability, and cells are therefore generally seeded onto pre-fabricated scaffolds[152]. This can be problematic as fibre mats, such as those created by electrospinning, are typically dense, therefore limiting the ability to seed cells homogeneously[151]. While methods for increasing porosity have been investigated to circumvent this, these methods intrinsically alter scaffold structure, placing limits on the range of structures that can be investigated in a disease modelling context[153]. While cell-compatible electrospinning methods do exist, these are often limited by cell viability as many key parameters such as electric field strength, flow rate and the chosen solvent for polymer dissolution can cause cell death[158]. FiberGel is cell compatible, yet the range of fibre diameters achievable are relatively thick compared to some of the nm-scale fibrillar structures found in tissues[159].

Moreover, it is relatively difficult to electrospin natural materials[149]. While reports of electrospinning collagen do exist, there are concerns regarding the loss of the native triple helix structure during the electrospinning process, even when using relatively gentle solvents such as acetic acid and ethanol[160]. As a result, 3D electrospun scaffolds are often fabricated from synthetic polymers, before including natural materials to enhance cell adhesion[160–162]. A recent study demonstrated the incorporation of a fibronectin within an electrospun microfibrous poly(lactide-co-glycolide) (PLG) scaffold, by inducing fibrillogenesis at the interface between the scaffold, the air and the fibronectin solution. These scaffolds enhanced engraftment efficiency in a mouse model of breast cancer, and improved *ex vivo* expansion of patient derived breast cancer cells[163].

Alternatively, synthetic and natural electrospun fibres can be functionalized with cell adhesive peptides such as RGD sequences for cell attachment[164,165]. Further, magnetic particles can be embedded within RGD-modified electrospun dextran vinyl sulfone (DVS) fibres and manipulated to control fibre orientation during gelation within the DVS hydrogel by applying a magnetic field[164]. This method recently showed that aligned architectures produced more unidirectional tendon cell (tenocyte) spreading and increased directional migration of breast cells from an encapsulated spheroid. Such composite systems, assembling pre-deposited fibres along with cells within a second system, hold promise for expanding the range of fibre architectures currently achievable by classical fibre-by-fibre deposition methods.

[H2] Porous scaffolds

Porous scaffolds form another class of biomaterials, encompassing a much wider range of porosity and pore size than is achievable in hydrogels. By some definitions, hydrogels can be considered a subcategory of porous scaffolds, although since their fabrication method is distinct, we will consider them separately. Many porous scaffolds typically contain pore sizes above the cell diameter, unlike hydrogels, which more commonly have pores smaller than the size of the embedded cells[166]. They also tend to be 'sponge-like', with rounder or thicker pores relative to hydrogels or fibrous scaffolds[167]. They may contain heterogeneous structures with a range of pore sizes (sometimes referred to as macro- and micro-porosity), which may mimic the hierarchical nature of some native tissues[168]. This can be accomplished through techniques such as gas foaming, where high pressure gas creates porosity by generating bubbles[169], or porogen leaching, where additives such as salt crystals are incorporated into the biomaterial mix and dissolved after formation[170]. Methods for creating and controlling porous scaffold structures are wide-ranging and their applicability to natural and synthetic materials varies with each technique, as has been discussed extensively in previous reviews on the topic[170–173].

One of the earlier examples of porous scaffolds in cancer research demonstrated the use of PLG as a 3D model of oral SCC. This model had pore sizes greater than 100 µm, and recreated the in vivo tumour growth profile of oral SCC, triggering the release of similar angiogenic factors[7]. More recently, primary PDAC cells grown in scaffolds created from primarily synthetic polymer formulations, either by particle-leaching or freeze-drying[167], formed a duct-like morphology similar to the tumour tissue. A similar morphology was not seen in synthetic fibrous scaffolds.

[H3] Incorporating control over fibre architecture

Although such scaffolds clearly have applications in cancer research, one downside is that many of the techniques used to induce porosity result in smooth, rounded pore walls. Although these may contain some level of micro- or nano-porosity, generally this is not representative of the 3D fibrous architecture of the ECM of soft tissues and tumours[174,175]. A fibrous component can, however, be introduced, for example by coating the scaffolds with ECM-derived proteins. When ECM-coated PCL scaffolds, generated using salt leaching and gas foaming, were implanted subcutaneously into mice bearing primary mammary carcinomas, the ECM-coated scaffolds showed enhanced colonisation by the cancer cells relative to uncoated scaffolds[176]. Another study created macroporous PLA scaffolds by incorporating PLA nanofibers into the pore walls to mimic collagen structure[175]. This was achieved using paraffin spheres as a porogen, and thermally-induced phase separation to create 50–500 nm fibres within the pore walls. Interestingly, these nanofibers were found to adsorb proteins such as fibronectin and vitronectin from the serum-containing medium, indirectly enhancing cell attachment in culture.

Ice-templating provides superior control over fibre architecture and has been extensively studied in tissue engineering but only recently adopted in cancer research (Fig. 3B). This induces porosity through the crystallisation of ice, thereby allowing control over fibre architecture by carefully tuning ice crystallisation kinetics[177–179]. For example, applying a thermal gradient across a collagen suspension causes directional ice crystal growth, leading to aligned collagen channels, whereas a more homogeneous freezing profile creates more rounded pores[180]. The nature of ice crystallisation means that collagen is excluded from the freezing water, becoming trapped between the ice crystals to form a negative replica of the ice crystal network. This approach has been routinely used in tissue engineering to create tissue-mimetic structures, which can include controlled architectural gradients[181,182]. Ice-templated scaffolds have been applied to study the relationship between breast cancer cell line invasion and proliferation, noting an increase in proliferation at the leading edge[183]. Therapeutic responses of tumour segments from MMTV-Wnt1 mouse models of cancer have also been examined in collagen scaffolds designed to mimic TACS-3 structures, combined with pre-adipocyte co-culture, examining cell invasion over several mm using tissue clearing technology[184].

[H3] Limitations and future directions

Many fabrication techniques for porous scaffolds have so far been designed to yield pore size ranges suitable for tissue engineering, typically between 20-120 µm for dermis[185], and between 100-500 µm for cartilage and bone, though larger pore sizes have also been investigated[186,187]. This restricts their application given that cancerous tissue can contain pore sizes of less than 5 µm[188]. Techniques do exist for smaller pore size fabrication, such as ice-templating[181], however, the relative paucity of studies replicating features at this scale warrants further study. Recent materials science studies have shown the link between scaffold structure and thermal profile during ice solidification, facilitating the controlled design of bespoke pore structures[189,190]. Application of ultrasound for improved control over fibre nucleation also overcomes one of the traditional downsides of ice-templating, the batch-to-batch variation that occurs due to stochastic ice crystal nucleation[191].

Many techniques for fabricating porous scaffolds are not cell compatible, due to the harsh temperatures or solvents used[192,193], although unlike electrospun scaffolds, porous scaffold microarchitectures that are permissible to cell colonisation post-fabrication may be readily designed allowing efficient cell seeding and colonisation[194]. Porous collagen-based scaffolds may also now also be fabricated in medium-throughput arrays using ice-templating, in a set-up compatible with fluorescent readouts of cell behaviour, allowing the dual influences of scaffold microstructure and biomolecular gradients to be probed[195].

[H2] Decellularised matrices

Decellularised matrices are derived from animal tissue, human tissue or cell cultures, and is treated to remove the cells while preserving ECM composition and/or architecture[196,197]. In the case of animal- or human-derived tissue and depending on the protocol used, the resulting tissue may be seeded with cells in its native state or may be milled and reprocessed into a natural hydrogel or coating[198,199]. A similar process can be used to extract biomaterials from ECM deposited by stromal cells cultured *in vitro*, with the resulting structures termed cell-derived matrices (CDMs)[200]. ECM deposition may be promoted *in vitro* by supplementing the media with ascorbic acid (an essential cofactor for collagen biosynthesis), adding macromolecular crowding agents, or using physical supports as templates for ECM deposition such as poly-lactic acid (PLA) microcarriers[201,202] (Fig. 3B). Both decellularized tissue and CDMs retain a complex ECM biochemical composition characteristic of the tissue or cell type of origin, however since their composition is typically heterogeneous, it requires characterization to delineate ECM contribution to the phenotype under study[203].

[H3] Manipulation of fibre networks by cellular remodelling

When decellularized matrices are used to produce hydrogels, many of the previously discussed techniques for controlling fibre networks are applicable. The resulting hydrogel may retain some structural characteristics of the original ECM, as reviewed elsewhere[204], which could be advantageous if using patient-derived ECM from the tissue of interest, but potentially limiting for alternative ECM sources (Fig. 3A). When CDMs are used in their native state, a 'guiding template' can be used to manipulate the properties of the cell-deposited fibre network. For example, a PDMS film containing micro-sized grooves induces alignment of collagen and fibronectin deposited by cultured fibroblasts, absent from ECM deposited on unpatterned PDMS, as assessed with second harmonic generation (SHG) imaging and immunostaining[203]. Although relatively thin at 20 µm, these matrices may nevertheless be used to compare cell migration dynamics in disordered versus aligned 3D fibre architectures[205,206].

Further work has shown that ECM alignment may also be induced by tissue maturation within moulds of defined aspect ratio (AR). After 5 weeks of culturing fibroblasts seeded into gelatin microparticles in a bioreactor, a more aligned ECM was produced by fibroblasts confined in moulds with an AR of 50, relative to ECM produced in a mould with an AR of 1[207]. Similarly, fibroblast seeding around an agarose plug can induce ECM deposition under tension[208], generated by the circumferential cytoskeletal forces that occur through cell-cell adhesion and alignment around the plug. Release from the plug induced relaxation of the fibroblast-deposited ECM, creating a crimped collagen structure resembling that seen in fibrotic tissues. Cell seeding density and media composition could be modified to tune the ECM properties further, with higher amounts of foetal bovine serum leading to lower stiffnesses whilst retaining constant collagen concentrations

[H3] Limitations and future directions

Like many naturally derived matrices, cell-deposited ECM has batch-to-batch variation but compensates for this with other advantages. These include more *in vivo* realistic composition and organisation relative to synthetic or single-component natural materials, as well as the capability of transferring long range mechanics[200,209]. A potentially larger concern is the limited size and scale-up of these CDMs, and due to their thickness they are sometimes considered 2.5D culture systems rather than truly 3D[210,211]. Techniques such as macromolecular crowding agents and bioreactors (reviewed elsewhere)[212] can improve the yield of CDM systems, however the cell expansion needed to increase CDM yields can be laborious and costly. Furthermore, these approaches do not allow for a premeditated design and so rely on post-generation analysis to map their resulting architecture.

An alternative approach is to encapsulate contractile cells within a synthetic or naturally derived hydrogel. Cells encapsulated in synthetic hydrogels, including breast cancer cell lines and patient-derived breast cells, have been shown to deposit additional ECM components specific to their tissue of origin, and to modify local ECM protein arrangement[17,213]. Another example of this approach is the organotypic assay, which is based on the premise that fibroblasts remodel a collagen gel into a matrix resembling their tissue of origin[214]. This has been validated by histological similarities to the native tissue in terms of cell organisation[215], however, to our knowledge the precise structural features of such matrices have not been validated. As with CDMs, there is limited control over the resulting matrix architecture.

Fibre remodelling on a similar scale to that in collagen gels has also been recently observed in synthetic hydrogels[93] and in synthetic fibre networks[216]. In methacrylated dextran fibre networks generated through combined electrospinning and lithography, mesenchymal stem cell-matrix interactions and

remodelling were similar to the levels seen in collagen gels. Importantly electrospinning provided additional control over fibre network parameters[216], indicating the possibility of combining several of the approaches discussed here as a route towards superior control over fibre architectures.

[H2] 3D bioprinting approaches

For the purposes of this review, we consider the term "3D bioprinting" to encompass any additive manufacturing **[G]** technique applied to biological materials, as reviewed in detail previously[217]. This encompasses methods that deposit materials using a print head or similar technology, as well as light-activated polymerisation[218].

[H3] Patterning fibre networks by 3D bioprinting

3D bioprinting may be used to impart highly defined, regular architectural features into a biomaterial. Typically, these structures are computationally pre-defined before synthesising. Synthesis methods include extrusion, inkjet bioprinting (printing drop-by-drop), and stereolithography (layer-by-layer photopolymerisation)[219]. Of these, light-based techniques typically offer the greatest resolution, particularly multiphoton polymerisation, which can achieve sub-micron resolution. This technique uses a laser to polymerise a light-responsive biomaterial **[G]**, creating patterns such as meshes with defined pore size[220]. This has been used to demonstrate that migrating HT1080 fibrosarcoma cells decreased in migration speed and persistence in lower pore size matrices (down to 12.5 µm)[221], and to define the pore sizes needed for various breast cancer cell lines to invade[220].

Although multiphoton polymerisation can achieve resolutions of as little as 0.5 µm[220,222], it is generally slower, with a lower throughput, and less suited to multicomponent printing than lower resolution techniques such as extrusion and inkjet bioprinting[219,223]. These lower resolution techniques often have the advantage of faster fabrication and therefore better maintenance of cell viability[223]. One bioprinting technique with intermediate resolution is cell electrowriting, which has been used to fabricate silk fibroin and gelatin-based fibres with diameters of 40–45 µm and 3–6 µm respectively[224]. This enabled printing of cells encapsulated within the gels while tuning fibre properties such as diameter, curvature, and straightness. The main limitation was the relatively small size of the constructs achievable, with a maximum thickness of 200 µm for silk-based and 50 µm for gelatin-based scaffolds. The loss of printing resolution at greater thicknesses was hypothesised to be a result of charge accumulation from the electrowriting process. It is possible that this size limitation may limit application of these constructs for some applications, such as 3D cell cluster cultures or long-range migration studies.

[H3] Limitations and future directions

As techniques advance, validating the final printed structures will be crucial. Although precise fabrication is possible, especially at submicron resolution, it is essential to confirm whether the theoretical resolution provided by the optics of the system matches the results. As noted previously, soft materials may produce distortions, while light penetration and photochemistry can limit true resolution, indicating a need for thorough evaluation of the printed scaffold to ensure reproducibility (Fig. 1)[219,225].

There is often a trade-off between the resolution and throughput in 3D bioprinting, constraining both the size of the constructs and the production speed. Multiphoton printing is particularly limited by its slow speed and low throughput, with a typical 1 cm x 1 cm x 100 µm structure requiring over a week to print due to the fabrication by laser point-by-point scanning[226]. While advances for multiphoton 3D printing have improved scalability of printing synthetic polymers, translation of these methods to

bioprinting is challenging due to the aqueous environment required and the photosensitivity of biological materials[226–228]. However, multiple laser foci have been implemented to create 3D materials for stem cell culture, indicating future potential for application to 3D cancer models[225], while new advances in bioinks with high reactivity also allow faster printing while maintaining biocompatibility[229].

A promising alternative technique, allowing control of 3D structure within hydrogels of dimensions over 10 mm, is filamented light (FLight) biofabrication[230,231]. This uses a projected light beam[231], which breaks up into multiple filaments as it enters a photoresponsive material, such as methacrylate- or norbornene-modified gelatin or hyaluronic acid, to induce photocrosslinking. Using this method, crosslinked microfilaments with diameters between 2 and 30 µm can be produced in seconds, with corresponding pore sizes between 3 and 14 µm[230]. Although structures with pore sizes above 5.8 µm have been shown to guide fibroblast migration[231], to our knowledge, pore sizes larger than 14 µm have not yet been explored, and certainly not in the cancer space.

Fibre length and alignment in cell-containing collagen networks can also be tuned by combining microextrusion, a relatively low resolution bioprinting method, with control over gelation kinetics[232]. This is achieved using additions that allow the collagen to be stably extruded without disrupting its self-assembly, such as Matrigel, and by controlling nozzle exit diameter and printing pressure/speed. This allowed complex multidirectional alignment of collagen fibres with a diameter 1-2 µm, despite an actual print resolution of 600 µm, demonstrating that control of collagen self-assembly may be successfully combined with 3D bioprinting methods.

[H2] Application of microfluidics

Microfluidics, a technology manipulating fluid flow through microchannels of highly-defined geometry, is an alternative approach for studying how specific features affect cell behaviour. It enables investigation of cellular responses to channel width or shear stress, akin to the fibrotic tumour microenvironment[233,234]. For example, a study used a polydimethylsiloxane (PDMS) microfluidic device to study cancer cell migration in narrow channels, facilitating attachment through inclusion of collagen or fibronectin[235]. While not directly controlling fibre architecture, such approaches nevertheless allow for reproducible study of cell behaviour in response to architectural features resembling key tumour tissue features.

A subcategory of microfluidic devices, designed to mimic a particular tissue, may be referred to as an organ on a chip, or ‘organ chip’. These are generally more complex, and may incorporate multiple channels, an air-liquid interface (e.g. for lung cancer modelling) and multiple ECM proteins and cell types[234]. These devices may incorporate hydrogels, allowing for control of fibre networks within them. Alternatively, microfluidics can be used to pattern fibre networks, as seen in a study patterning fibres of various alignments in collagen within microfluidic channels of different widths[236]. Previous reviews further discuss the use of microfluidics for modelling responses to geometrical features in the tumour microenvironment[233,234].

[H1] Informing tissue-specific model design

While the end goal of the techniques summarised above is to produce 3D models that reproduce key features of the tumour microenvironment, achieving this requires detailed knowledge of the tissue-specific fibre architecture. While certain fibre characteristics correlate with clinical outcome, fully recapitulating tumour fibre structures with biomaterials remains a challenge. Here, we highlight techniques with the potential to accurately map the tumour ECM, facilitating translation towards tissue-mimetic biomaterial design (Fig. 1).

[H2] Imaging 3D fibre organisation from patient-derived tissue

Histological staining of formalin-fixed paraffin-embedded (FFPE) patient derived tissue sections, using haematoxylin and eosin (H&E), Masson's Trichrome and picrosirius red (PSR), provides an overview of the protein and cellular compartments in the tissue and visualisation of the connective tissue[237]. While PSR is not intrinsically specific to collagen, it binds to collagen fibres, increasing the natural birefringence for structural analysis when imaged under polarised light. Although the resolution is typically not at the level of the individual fibre, these methods may be used to assess collagen bundle orientation with high efficiency and reproducibility in large samples[238]. Similar staining methods also exist with more specificity to individual ECM components, such as antibody-based immunofluorescence staining and collagen binding peptides[239].

Although generally used for 2D imaging, archival FFPE material (5-10 µm thick sections) holds potential for extensive mapping of 3D fibre architecture and a recent tutorial described the considerations for extracting 3D information[240]. One approach is to create serial sections from the FFPE block, followed by sequential imaging and 3D image alignment to generate a volumetric image. Another approach is to visualise the entire block without sectioning, using tissue clearing followed by light-sheet microscopy, or X-ray Micro-Computed Tomography (Micro-CT) **[G]**. Care should be taken, however, if implementing these protocols for the study of fibre organisation, since some tissue fixation and clearing protocols involve collagen dissociation, degradation and/or disruption[241].

Generally, there is an inverse correlation between the penetration depth into the tissue and the resolution achievable by a given technique[242]. For example, Micro-CT allows non-destructive imaging through entire cm^3 samples, but at the cost of lower resolution (~µm range). However, correlating Micro-CT with physical tissue sectioning and histology could be a powerful means of evaluating and validating 3D tissue architecture[243]. This approach of combining multiple imaging technologies at different length scales has also been implemented for the characterisation of ovarian tissue[244]. Combining scanning electron microscopy (SEM) **[G]**, atomic force microscopy **[G]**, and various histological stains demonstrated key changes in fibre network characteristics between prepuberty, reproductive age and menopause, at different length scales. Although an intrinsically 2D surface technique, SEM can provide 3D fibre information, although this is typically destructive and often laborious[244,245].

A widely-accepted and specific approach for imaging 3D collagen fibres is second harmonic generation (SHG) imaging. This is a high-resolution 2-photon optical microscopy technique that specifically detects non-centrosymmetric biomolecules such as fibrillar collagen[246]. Unlike other imaging methods based on native autofluorescence or fluorescent stains, this technique has the capability to isolate and image only the fibrillar collagen playing a structural role in the tumour fibre architecture. SHG imaging originally defined TACS in breast cancer (Fig. 2A)[46,47], indicating its capability for identifying key fibre patterns and thus informing the design of 3D biomaterial models. Its key features are that it is non-destructive and stain-free, allowing high imaging depth into 3D tissue.

SHG imaging does, however, require specialised equipment. This has led to the development of an alternative and cheaper label-free system, liquid crystal-based polarisation microscopy (LC-PolScope). SHG imaging and LC-PolScope analysis show good agreement in quantifying breast and pancreatic tissue organisation from histological sections of patient tissue samples[247]. LC-PolScope however is limited in that it can only image thin samples, and requires time-consuming serial sectioning, imaging and analysis to understand 3D topology. In contract, SHG imaging excels in 3D sample analysis by imaging deep with minimal loss of resolution, offering a deeper understanding of native 3D structure[246].

Other 3D label-free techniques include Raman microscopy, which can offer similar resolution to two-photon fluorescence imaging[248]. This is potentially very powerful for informing biomaterial model design, since it has the capability to correlate composition and structure, and map the fibre architecture of specific biomolecular components.[249]. Such methods can identify the composition of biological samples based on molecular 'fingerprints' that arise based on each molecule's interaction with the incident light[250]. A recent study combined Raman spectroscopy and SHG imaging to investigate the makeup of fibrotic tissue[251], highlighting again the potential of multimodal imaging to maximise output.

[H2] Image analysis approaches for quantifying fibre architecture

Gray level co-occurrence matrix (GLCM) analysis of SHG imaging data is an example of a texture-based analysis that quantifies similarities in structures according to properties of the fibre network[246]. Textural variations, stemming from factors such as fibre density, width and length, require careful interpretation for meaningful biological understanding. Although GLCM analysis is limited to 2D quantification, another method, Fiber-Analysis-Algorithm, allows 3D texture analysis using machine learning to categorise SHG images of various tissues, according to a wide range of matrix structural parameters[252,253].

While these methods allow categorisation of images according to global patterns, they do not provide quantification of individual fibre parameters. Several software-based tools have been developed for this purpose, including The Workflow Of Matrix BioLogy Informatics (TWOMBLI), which allows a number of "matrix metrics" to be extracted, both those describing individual fibres and those describing general ECM patterning, which can feed into biomaterial design[254]. TWOMBLI is often used for quantifying histological stains such as PSR, including patient tissue sections and sectioned biomaterials[211,255]. Conversely, CurveAlign, which measures the overall trend in fibre alignment, and CT-Fire, which allows extraction of individual fibre parameters such as straightness, thickness and curvature, are commonly used for SHG image data[42]. TWOMBLI and CurveAlign currently only support 2D image analysis, although CT-Fire does have the capability to extend the same methods to 3D[256].

Quantifying 3D data is crucial for accurately assessing fibre architecture, as 2D data can be affected by artefacts in fibre orientation[252]. Emerging methods for 3D fibre parameterisation include MatLab codes allowing quantification of 3D fibre orientation, diameter and branching from image data including multiphoton and SHG imaging[253]. Standalone, open-source packages are also available, such as Foa3D for 3D fibre orientation analysis[257], and VesselExpress and VesselVio, originally designed for quantification of vascular network parameters[258,259], and may also apply to fibre network parameterization. Together, these programs allow extraction of many different parameters that can describe fibrous tissue networks. While some of these parameters have known links to cancer outcome, such as fibre diameter[53], others, such as branchpoints and tortuosity, remain unexplored. Understanding whether these relatively unstudied structural parameters also play a role in cancer progression remains a key question.

[H2] Mapping tissue-specific 3D fibre organisation into biomaterials

Combined with advances in biomaterials synthesis technology (Fig. 3C), the ability to recreate key 3D architectural features within tissue-mimetic biomaterials is now tangible. One recent example applied multiscale imaging to characterise fibre diameter, pore size and fibre orientation in healthy and diseased ovarian tissues, to create age-specific models[244]. Using collagen–GelMA structures, the fibre networks were replicated and ovarian cell migration dynamics were assessed in response to the various fibre architectures[222]. Here, the structures were 10 μm in thickness, however if this could be

expanded to allow recreation of larger-scale 3D tissue structures, it could have broader applicability. While currently not feasible with multiphoton bioprinting due to its slow and labour-intensive process, techniques for increasing its speed and throughput are rapidly expanding. Such methods are now being applied to reproduce SHG image data with high fidelity in biomaterials, reducing printing time from a week to 2 days[226]. Such speed enhancements, coupled with accurate recapitulation of 3D topology, will greatly assist in the implementation of these approaches into general cancer research.

While it seems that the goal of reproducing the exact features of tumour ECM is indeed achievable, and advances are constantly being made in this area, it should be considered that many of the methods required to do this, such as the two-photon polymerisation method, will likely remain relatively time-intensive, expensive, and require the use of specialised equipment. It is therefore likely that a balance will need to be struck between the complexity and fidelity of the biomaterial design, and its ease of use and reproducibility between labs. One approach for model standardisation is to parameterise the key structural features of tissue fibre architecture, allowing this to be more readily reproduced between labs (Fig. 1). For instance, fibre shapes in ovarian tissue at different disease stages have been modelled as sine waves[222], shapes which may be easier to replicate using faster, higher-throughput techniques.

The scalability and reproducibility of biomaterial design may also be enhanced using 3D printed templates or moulds. For instance, a simple but innovative method of controlling collagen alignment uses 3D printable wedges that incline collagen-coated coverslips to a controlled degree, relying on gravity to generate reproducible alignment within the resulting collagen matrix[260]. Similarly, others have created a modular, 3D-printable system to create thermal gradients for application to ice-templating, which could be adopted without the need for specialised equipment[261]. Another study parameterised gradients in collagen fibre orientation from SHG images of breast cancer and reproduced them in collagen gels using a microfluidic system with an intentionally reproducible design to allow its use by other research laboratories[262].

[H1] Conclusions and Future Perspectives

Current research in the fields of biomaterials and 3D image characterisation is rapidly progressing towards a stage where precise models of tumour fibre architecture can be utilized widely. While models of controlled stiffness and ECM composition are available, the addition of biologically realistic fibre organisation will enhance the design of tissue-realistic models, impacting both basic science and drug discovery. We suggest that moving forward, detailed tissue imaging and fibre network parameterisation could inform the design and fabrication of advanced biomaterials with tissue realistic structure, followed by imaging of the biomaterial structures themselves to enable correlation to the original tissue (Fig. 1). With the emergence of such biomaterial technologies allowing 3D architectural control, it will soon be possible to elucidate, functionally test and validate the key roles of ECM organisation in cancer development, drug response and eventual patient outcome. Additionally, tissue-specific biomaterials could help to predict therapeutic efficacy, ultimately aiding in patient stratification to enhance the likelihood of therapeutic success.

Moreover, these advanced biomaterials could also have potential applications in precision medicine. Recent studies have applied biomaterial models for the expansion and culture of patient-derived material from patients with breast and pancreatic cancer, controlling for ECM stiffness, composition and fibre alignment[213,263]. Based primarily on animal-free biomaterials technology, these methods could replace, reduce, and refine the use of reagents such as Matrigel for maintaining and expanding patient-derived organoids. Furthermore, engineering patient-specific biomaterials based on combined analysis of tissue composition and structure is a promising approach. The development of

Raman and mass spectrometry imaging methods for spatial mapping of ECM composition, combined with new techniques for 3D patterning biomaterial functionalisation[264], could potentially lead to combined spatial control over ECM fibre structure and composition in highly advanced precision biomaterials. While there remain key outstanding questions in the field (Box 1), the future application of such precision biomaterials holds great promise to improve cancer outcomes. Through the coordinated efforts of interdisciplinary teams of materials scientists, cancer researchers and experts in tissue imaging and analysis, the once distant goal of patient-specific methods for drug screening is steadily advancing.

Glossary

Additive manufacturing – the process of building an object based on 3D data, usually layer by layer, encompassing methods that directly deposit materials using a print head or similar (commonly grouped together as "3D printing", as well as other techniques such as light-activated polymerisation.

Amorphous collagen – collagen molecules that are not organised into fibrous or fibrillar structures.

Anastomosis – A connection between two passageways, such as where two previously independent, discrete blood vessels subsequently join.

Atomic force microscopy – A technique used for mapping the atomic-scale topography of a surface by means of the repulsive electronic forces between the surface and the tip of a microscope probe moving above the surface.

Basement Membrane – Structure visible by light microscopy and, in addition to the basal lamina, that consist of layers that are typically secreted by cells from underlying connective tissue. Many basement membranes are rich in fibronectin.

Cell jamming – A collective cell behaviour observed in densely packed groups of cells such as tumours, where they exhibit solid-like properties akin to jammed granular materials.

Collective invasion – A mode of migration in which groups of cells move together as a cohesive unit through the surrounding extracellular matrix.

Extrusion – A printing approach in which a continuous strand of material is deposited.

Fibrillar – Indicates that a molecule or substance has formed, or is intrinsically capable of forming, elongated units i.e. fibres, which in the ECM are often hierarchical, containing structure on multiple length scales.

Light-responsive biomaterial – A biomaterial that can undergo reversible or irreversible changes in its properties or functions upon exposure to light.

Integrin switching – A process in which cells dynamically alters integrin expression, engagement and/or or activation. For example, during cancer metastasis, tumour cells may undergo integrin switching to acquire a more invasive phenotype, enabling them to detach from the primary tumour, invade surrounding tissues,

Interstitial matrix – The interstitial matrix generally contains a high level of structural proteins, where collagen I and fibronectin are the main components in many tissues.

Micro-CT – A non-destructive imaging technique that produces detailed three-dimensional images of objects at a microscopic scale.

Microtracks – Microtracks are narrow, often microscopic-scale pathways or channels within the 3D matrix structure, that can guide the movement or alignment of cells.

Scanning electron microscopy (SEM) – A high resolution imaging technique that deploys a focused beam of electrons to scan the surface of the sample.

Shear stress – A type of stress that is defined as force per unit area and is caused by forces acting parallel to a surface, leading to a deformation or displacement.

Tunnelling nanotubes (TNTs) – Actin-based membrane protrusions that form cell-cell contacts.

Acknowledgements

T.R.C. is supported by the National Health and Medical Research Council (NHMRC) of Australia and Cancer Council NSW (CCNSW). J.C.A. is funded by the University of Nottingham (Anne McLaren fellowship). Figures in the accepted manuscript were created with BioRender.com.

Competing Interests

The authors declare the following competing interests: J.C.A. is a co-founder, shareholder, and Scientific Advisory Board member of Peptimatrix Ltd. T.R.C declares no conflicts of interest.

Author contributions

The authors contributed equally to all aspects of the article.

Peer review information

Nature Reviews Cancer thanks E. L. Shan Fong, K. Killian and the other, anonymous, reviewers for their contribution to the peer review of this work.

Table of content summary:

While there has been increasing interest in developing models that mimic the tumour microenvironment (TME), these models often fail to replicate the complex 3D fibre architectures observed in tumours. Here, Ashworth and Cox address this, discuss the current design and fabrication challenges, and outline state-of-the-art biomaterial technologies useful for recreating tissue-specific 3D architectures in vitro.

853 **Table 1: A summary of the main techniques for controlling 3D fibre orientation in polymeric**
854 **biomaterials.**

Technique for controlling fibre architecture		Advantages	Disadvantages	Example references
	Altering collagen fibrillogenesis through parameters such as pH, temperature of gelation and collagen concentration	Can mimic the collagen-rich ECM found in many tissues. Fibre diameters up to 10 µm now achievable. Well-documented application for assessing cell migration response to structural features. Compatible with cell encapsulation.	Difficult to vary parameters individually Naturally derived material with batch-to-batch variability. Difficult to achieve the larger pore sizes and fibre diameters found in tissue (>10 µm).	79,106,134,136,144,265
	Aligning fibre structures in hydrogels by applying mechanical forces, magnetic fields, electric fields or fluid flow	Fibre diameters between 1 nm and 10 µm achievable. Application of force and/or fields readily produces fibre alignment. Many techniques are compatible with cell encapsulation. Combining different biomaterials facilitates independent variation of structural properties.	Difficult to achieve the larger pore sizes and fibre diameters found in tissue (>10 µm). Methods for controlling other fibre architectural features are relatively unexplored.	128,129,137–139,141
	Altering the characteristics of individual fibres as they are produced through electric fields (e.g. electrospinning), flow/extrusion rates or stretching	A very wide range of diameters achievable, nm – mm scale. Enhanced control may be achieved by combining with other techniques.	Often not compatible with cell encapsulation. Often restricted to synthetic materials due to harsh solvents	150,152,153,155,159,266

		New techniques emerging to incorporate natural materials.	and/or temperatures. Structures produced are typically dense and difficult to seed evenly with cells.	
	Controlling pore structure and therefore fibre structure using porogens such as ice, gas or salt.	Wide range of pore sizes achievable, from <5 µm up to mm. Well-established in tissue engineering with known routes for mimicking tissue structures (especially ice-templating). Heterogeneous and gradient structures can be achieved.	Smaller, nm-size fibres may be difficult to achieve. Techniques for patterning fibre shape so far relatively unexplored. Cells must be seeded after fabrication. Can be associated with batch-to-batch variation.	[7,166,176,181–183]
	Influencing the way cells in culture synthesise ECM or contract and remodel hydrogels using media additives or physical scaffolds.	Complex, tissue-realistic composition can be created including multiple ECM components. Produces histological similarity to native tissue. Cell-compatible, while also allowing for subsequent cell removal and/or seeding of different cell types.	Produces complex matrices that may vary batch-to-batch and are difficult to characterise fully. Slow, low-throughput technique that is difficult to scale up. Structures cannot be precisely defined.	[201–203,207,208,214]
	Creating computationally-defined structures using a 3D bioprinting technique (ranging from extrusion-based	Covers a very wide range of architectural features down to sub-micron resolution, with virtually any structural feature seen in native tissue	Balance must be made between resolution and throughput: highest resolution techniques (multiphoton	[220,222,224,229,231]

	methods to stereolithography).	achievable within this size range. Allows very precise definition of printed constructs with highly regular features or based on image data. A rapidly advancing field with new advances improving speed, resolution and biocompatibility. Many techniques are compatible with encapsulated cells.	polymerisation) typically take days to weeks to print each construct. Multiphoton printing requires complex equipment and technical expertise. Fibrillar collagen is often difficult to print and is typically mixed with other materials. Most techniques are not optimised to produce feature sizes smaller than 500 nm.	

**Table references include pertinent studies only and is not meant to be an exhaustive list*. The references given have been chosen to reflect particular relevance or potential application to cancer research.

Figures

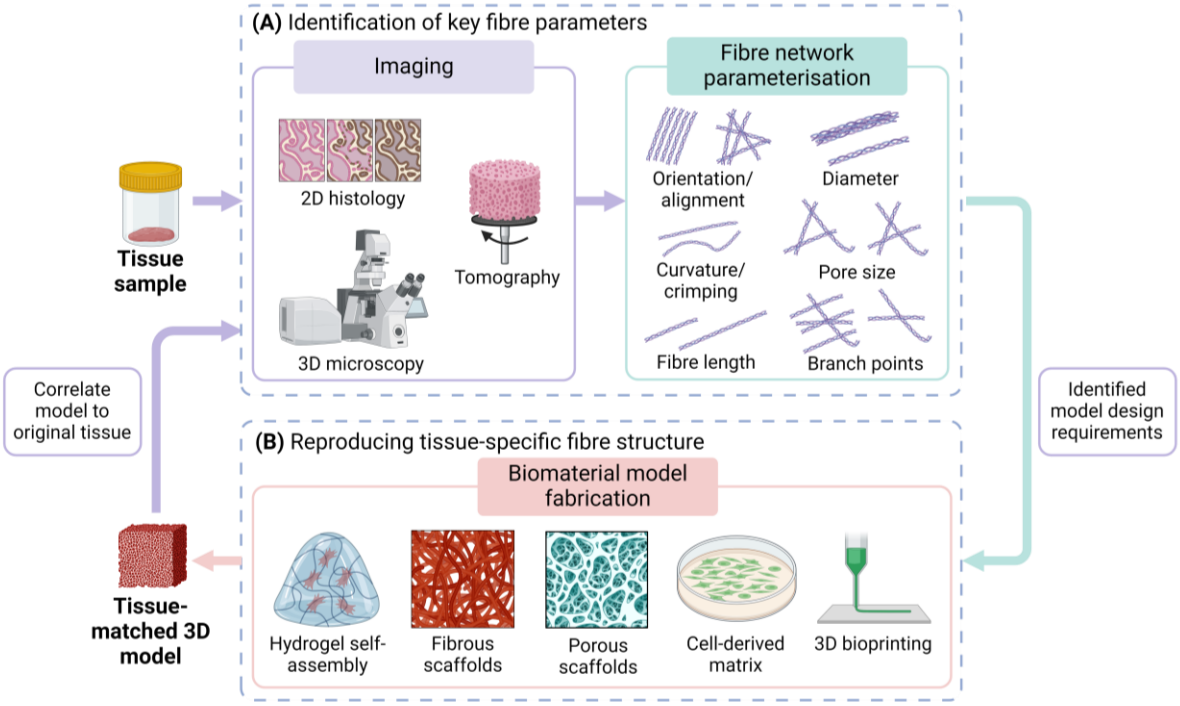

Figure 1: Approaches for designing and fabricating precision biomaterials with tissue-matched 3D fibre architecture. Patient-derived tissue samples, e.g. from surgery or biopsy, could in the future be imaged with the necessary accuracy and precision to allow (A) identification of key fibre network characteristics (e.g. fibre length, straightness) for (B) reproduction in a high-fidelity biomaterial. Via application of the same imaging approaches (e.g. histology, 3D microscopy), the characteristics of this biomaterial could then be correlated back to the original tissue, allowing fine-tuning and validation.

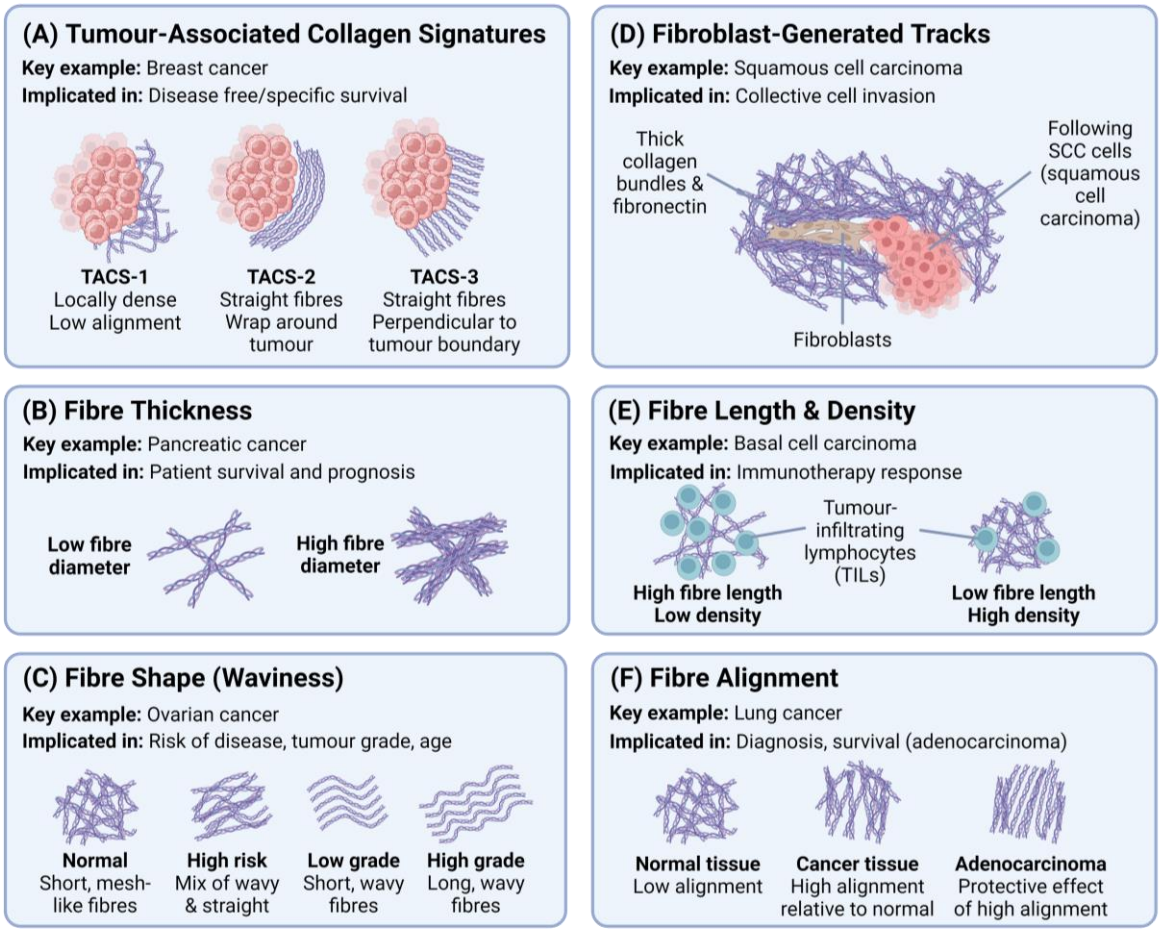

Figure 2: Fibre architecture varies across cancers of various origins, showing correlations with prognosis. These examples are not intended to be exhaustive, but to highlight the diversity in fibre patterns found to correlate with clinical outcome in a wide range of tissues. (A) TACS (tumour-associated collagen signatures) found primarily in breast cancer is linked to disease free/specific survival[46,47]; (B) fibre thickness is found to correlate to survival and prognosis in pancreatic cancer[53]; (C) fibre shape is found to correlate with risk of disease, tumour grade and age in ovarian cancer[50,51]; (D) fibroblast-generated tracks surrounded by thick collagen/fibronectin bundles have been linked to collective cell invasion in squamous cell carcinoma (SCC)[91]; (E) high fibre length and low density are found to correlate with infiltration of tumour-infiltrating lymphocytes (TILs) and immunotherapy response in basal cell carcinoma[96]; (F) fibre alignment is found to increase in lung cancer relative to normal tissue but has also been associated with improved survival specifically in adenocarcinoma[54].

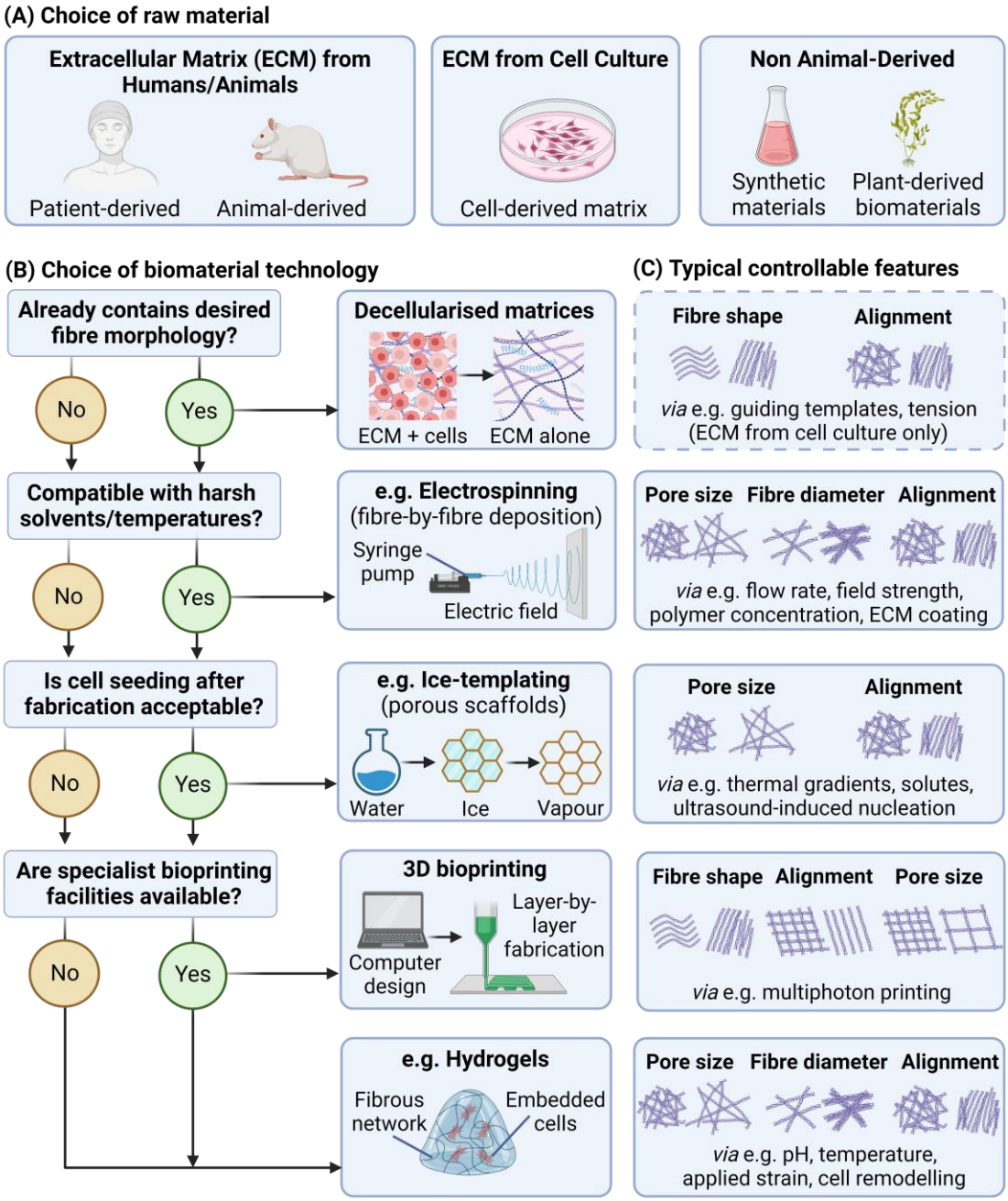

Figure 3: Approaches for control of fibre architecture through biomaterial fabrication. A) The initial choice of biomaterial raw material, along with other factors including B) the need for defined architecture beyond that found in native tissue, compatibility with harsh solvents and/or temperatures, the need for cell encapsulation during manufacture, and the availability of bioprinting technology will determine the choices of fabrication techniques available. C) Each technique is most suited to tuning distinct features. The typical fabrication parameters used to control such structural features are listed.

[b1] Box 1: 10 key outstanding questions in the field

1. What specific roles do key components of the extracellular matrix, such as collagens and fibronectin, play in regulating the genesis and maturation of matrix microarchitecture in the 3D tumour microenvironment?

2. How do alterations in the microarchitecture of the extracellular matrix contribute to the initiation and progression of different types of cancer, and do these changes interact with different mutational burdens in different ways.

3. To what extent does the interaction between cancer cells and the extracellular matrix microarchitecture influence the efficacy of conventional and contemporary cancer therapies and ultimately the development of acquired resistance?

4. Can targeting specific aspects of extracellular matrix architecture (or blocking cellular response to specific aspects) offer novel therapeutic strategies to impede cancer metastasis and improve patient outcomes?

5. Can the identification and validation of matrix architecture biomarkers aid in tailoring individualised treatment strategies and improving patient outcomes?

6. Can patient-mimetic models identify the relative importance of ECM stiffness, composition and fibre structure in determining patient outcome, and which should be the main focus of new therapies targeting the microenvironment?

7. Can tumour-specific fibre architectures be accurately recapitulated in biomaterial models to a sufficient extent that would allow application to precision medicine?

8. How accurately can complex structures such as tumour-margin boundaries and structural heterogeneity be replicated using biomaterials technology?

9. Can automated and robust workflows be developed for quantifying biologically meaningful features of the fibre networks in the tumour microenvironment, e.g. by application of machine learning?

10. What specific features of tumour fibre architecture are most important in determining patient outcome, and are these well-characterised structural features (e.g. fibre density, orientation) or features that are so far relatively unexplored (e.g. tortuosity, number of branchpoints)?

Key References

Alkmin, S. et al. Acta Biomater. 100, 92–104 (2019). **This study combines SHG imaging of ovarian tissue with multiphoton polymerisation to reproduce image data representing normal and tumor tissue, applying these constructs to study the role of fibre structure in migration dynamics.**

Baker BM et al. Nat Mater. 14(12), 1262-1268 (2015). This is a **study on cell response to microenvironmental stiffness in native-like extracellular matrices using engineered synthetic fibrous materials mimicking collagen matrices.**

Caballero, D., Palacios, L., Freitas, P. P. & Samitier, J. Adv. Funct. Mater. 27 (2017). **Cell-derived matrices, aligned using physical templates, are used in this study to demonstrate that fibre anisotropy dictates the directionality but not distance of cell migration.**

Cyr, J. A., Husmann, A., Best, S. M. & Cameron, R. E. Acta Biomater. 153, 260–272 (2022). **This study demonstrates application of multi-directional temperature gradients and finite element modelling to control and predict complex fibre architectures in ice-templated collagen scaffolds.**

Dobos, A. et al. Adv. Healthc. Mater. 9, e1900752 (2020). **This paper describes the development of a new bioink allowing rapid bioprinting of cell-containing materials by two-photon polymerisation.**

Freudiger, C. W. et al. Science 322, 1857–1861 (2008). **This paper describes Stimulated Raman Scattering microscopy for label-free in situ visualisation of 3D structures in living tissues.**

Levental KR et al. Cell. 139(5), 891-906 (2009). **This article demonstrates that collagen crosslinking and stiffening underpins breast tumourigenesis highlighting how collagen architecture influences breast cancer malignancy.**

Mayorca-Guiliani AE at al. Nat Med. 23(7):890-898 (2017). **Here, Mayorca-Guiliani et al. develop a new tissue decellularisation platform for high resolution characterisation of the 3D tumour matrix, including high resolution mapping of collagen architecture.**

Naba A et al. Molecular and Cellular Proteomics. 11(4), 1-18 (2012). **This paper details proteomic strategies to characterise normal and tumour extracellular matrix composition to facilitate broader application of these methods for studying disease.**

Pearce OMT et al. Cancer Discov. 8(3):304-319 (2018). This study **demonstrates that multi-omics characterisation of the evolving human metastatic microenvironment from patient samples can be**

used to define matrisome signatures distinguishing patients with a shorter overall survival in ovarian and 12 other primary solid cancers.

Provenzano et al. BMC Med. 26, 4(1), 38 (2006). This is a **landmark paper defining the three tumour-associated collagen signatures (TACS) that have since been shown to be diagnostic and prognostic of disease progression and outcome.**

Tian C. et al. Proc Natl Acad Sci USA 116, 19609–19618 (2019). This is the **first demonstration that individual matrisome proteins derived from pancreatic cancer stromal cells or from cancer cells differentially correlate with patient outcome.**

Velez, D. O. et al. Nat. Commun. 8, 1651 (2017). **This article demonstrates the application of molecular crowding to achieve independent control over fibre architecture and collagen hydrogel stiffness, to show that matrix architecture (pore size and fibre length) regulates β1-integrin signalling and cancer cell motility.**

Wolf, K. et al. J. Cell Biol. 201, 1069–1084 (2013). **This study describes the relationship between tumour fibre architecture and cell migration by identifying critical pore sizes at which migration is inhibited.**

Zeugolis, D. I. et al. Biomaterials 29, 2293–2305 (2008). **A key study demonstrating the difficulty in electrospinning natural materials, showing for the first time the loss of the collagen triple helix in electrospun constructs.**

References

1. Theocharis, A. D., Manou, D. & Karamanos, N. K. The extracellular matrix as a multitasking player in disease. *FEBS J.* **286**, 2830–2869 (2019).

2. Pickup, M. W., Mouw, J. K. & Weaver, V. M. The extracellular matrix modulates the hallmarks of cancer. *EMBO Rep.* **15**, 1243–1253 (2014).

3. Cox, T. R. & Erler, J. T. Remodeling and homeostasis of the extracellular matrix: implications for fibrotic diseases and cancer. *Dis. Model. Mech.* **4**, 165–178 (2011).

4. Daley, W. P., Peters, S. B. & Larsen, M. Extracellular matrix dynamics in development and regenerative medicine. *J. Cell Sci.* **121**, 255–264 (2008).

5. Naba, A. *et al.* The matrisome: in silico definition and in vivo characterization by proteomics of normal and tumor extracellular matrices. *Mol. Cell. Proteomics* **11**, M111.014647 (2012).

6. Chen, S. *et al.* Cancer-associated fibroblasts suppress SOX2-induced dysplasia in a lung squamous cancer coculture. *Proc Natl Acad Sci USA* **115**, E11671–E11680 (2018).

7. Fischbach, C. *et al.* Engineering tumors with 3D scaffolds. *Nat. Methods* **4**, 855–860 (2007).

8. Riedl, A. *et al.* Comparison of cancer cells in 2D vs 3D culture reveals differences in AKT-mTOR-S6K signaling and drug responses. *J. Cell Sci.* **130**, 203–218 (2017).

9. Yamada, K. M. & Cukierman, E. Modeling tissue morphogenesis and cancer in 3D. *Cell* **130**, 601–610 (2007).

10. Baker, B. M. & Chen, C. S. Deconstructing the third dimension: how 3D culture microenvironments alter cellular cues. *J. Cell Sci.* **125**, 3015–3024 (2012).

11. Caballero, D. *et al.* Precision biomaterials in cancer theranostics and modelling. *Biomaterials* **280**, 121299 (2022).

12. Curvello, R., Kast, V., Ordóñez-Morán, P., Mata, A. & Loessner, D. Biomaterial-based platforms for tumour tissue engineering. *Nat. Rev. Mater.* (2023) doi:10.1038/s41578-023-00535-3.

13. Sievers, J., Mahajan, V., Welzel, P. B., Werner, C. & Taubenberger, A. Precision hydrogels for the study of cancer cell mechanobiology. *Adv. Healthc. Mater.* **12**, e2202514 (2023).

14. Mullard, A. R&D re-balancing act. *Nat. Rev. Drug Discov.* **22**, 258 (2023).

15. Brancato, V., Oliveira, J. M., Correlo, V. M., Reis, R. L. & Kundu, S. C. Could 3D models of cancer enhance drug screening? *Biomaterials* **232**, 119744 (2020).

16. Rodenhizer, D., Dean, T., D'Arcangelo, E. & McGuigan, A. P. The current landscape of 3D in vitro tumor models: what cancer hallmarks are accessible for drug discovery? *Adv. Healthc. Mater.* **7**, e1701174 (2018).

17. Ashworth, J. C. *et al.* Peptide gels of fully-defined composition and mechanics for probing cell-cell and cell-matrix interactions in vitro. *Matrix Biol.* **85–86**, 15–33 (2020).

18. Gjorevski, N. *et al.* Designer matrices for intestinal stem cell and organoid culture. *Nature* **539**, 560–564 (2016).

19. Micalet, A., Moeendarbary, E. & Cheema, U. 3D in vitro models for investigating the role of stiffness in cancer invasion. *ACS Biomater. Sci. Eng.* **9**, 3729–3741 (2023).

20. Sokol, E. S. *et al.* Growth of human breast tissues from patient cells in 3D hydrogel scaffolds. *Breast Cancer Res.* **18**, 19 (2016).

21. Bonnans, C., Chou, J. & Werb, Z. Remodelling the extracellular matrix in development and disease. *Nat. Rev. Mol. Cell Biol.* **15**, 786–801 (2014).

22. Winkler, J., Abisoye-Ogunniyan, A., Metcalf, K. J. & Werb, Z. Concepts of extracellular matrix remodelling in tumour progression and metastasis. *Nat. Commun.* **11**, 5120 (2020).

23. Sahai, E. *et al.* A framework for advancing our understanding of cancer-associated fibroblasts. *Nat. Rev. Cancer* **20**, 174–186 (2020).

24. Malik, R., Lelkes, P. I. & Cukierman, E. Biomechanical and biochemical remodeling of stromal extracellular matrix in cancer. *Trends Biotechnol.* **33**, 230–236 (2015).

25. Lee, S. *et al.* Differentially expressed genes regulating the progression of ductal carcinoma in situ to invasive breast cancer. *Cancer Res.* **72**, 4574–4586 (2012).

26. Naba, A., Clauser, K. R., Lamar, J. M., Carr, S. A. & Hynes, R. O. Extracellular matrix signatures of human mammary carcinoma identify novel metastasis promoters. *eLife* **3**, e01308 (2014).

27. Tian, C. *et al.* Proteomic analyses of ECM during pancreatic ductal adenocarcinoma progression reveal different contributions by tumor and stromal cells. *Proc Natl Acad Sci USA* **116**, 19609–19618 (2019).

28. Tian, C. *et al.* Cancer Cell-Derived Matrisome Proteins Promote Metastasis in Pancreatic Ductal Adenocarcinoma. *Cancer Res.* **80**, 1461–1474 (2020).

29. Ting, D. T. *et al.* Single-cell RNA sequencing identifies extracellular matrix gene expression by pancreatic circulating tumor cells. *Cell Rep.* **8**, 1905–1918 (2014).

30. Vargas, A. C. *et al.* Gene expression profiling of tumour epithelial and stromal compartments during breast cancer progression. *Breast Cancer Res. Treat.* **135**, 153–165 (2012).

31. Chitty, J. L. *et al.* A first-in-class pan-lysyl oxidase inhibitor impairs stromal remodeling and enhances gemcitabine response and survival in pancreatic cancer. *Nat. Cancer* **4**, 1326–1344 (2023).

32. Levental, K. R. *et al.* Matrix crosslinking forces tumor progression by enhancing integrin signaling. *Cell* **139**, 891–906 (2009).

33. Liu, D. & Hornsby, P. J. Senescent human fibroblasts increase the early growth of xenograft tumors via matrix metalloproteinase secretion. *Cancer Res.* **67**, 3117–3126 (2007).

34. Shinde, A. *et al.* Tissue transglutaminase expression promotes cell attachment, invasion and survival in breast cancer cells. *Oncogenesis* **9**, (2020).

35. Shinde, A. *et al.* Transglutaminase-2 facilitates extracellular vesicle-mediated establishment of the metastatic niche. *Oncogenesis* **9**, 16 (2020).

36. Acerbi, I. *et al.* Human breast cancer invasion and aggression correlates with ECM stiffening and immune cell infiltration. *Integr Biol (Camb)* **7**, 1120–1134 (2015).

37. Goetz, J. G. *et al.* Biomechanical remodeling of the microenvironment by stromal caveolin-1 favors tumor invasion and metastasis. *Cell* **146**, 148–163 (2011).

38. Provenzano, P. P., Inman, D. R., Eliceiri, K. W., Trier, S. M. & Keely, P. J. Contact guidance mediated three-dimensional cell migration is regulated by Rho/ROCK-dependent matrix reorganization. *Biophys. J.* **95**, 5374–5384 (2008).

39. Conklin, M. W. *et al.* Collagen Alignment as a Predictor of Recurrence after Ductal Carcinoma In Situ. *Cancer Epidemiol. Biomarkers Prev.* **27**, 138–145 (2018).

40. Piersma, B., Hayward, M.-K. & Weaver, V. M. Fibrosis and cancer: A strained relationship. *Biochim. Biophys. Acta Rev. Cancer* **1873**, 188356 (2020).

41. Brauchle, E. *et al.* Biomechanical and biomolecular characterization of extracellular matrix structures in human colon carcinomas. *Matrix Biol.* **68–69**, 180–193 (2018).

42. Bredfeldt, J. S. *et al.* Computational segmentation of collagen fibers from second-harmonic generation images of breast cancer. *J. Biomed. Opt.* **19**, 16007 (2014).

43. Guo, Y. P. *et al.* Growth factors and stromal matrix proteins associated with mammographic densities. *Cancer Epidemiol. Biomarkers Prev.* **10**, 243–248 (2001).

44. McCormack, V. A. & dos Santos Silva, I. Breast density and parenchymal patterns as markers of breast cancer risk: a meta-analysis. *Cancer Epidemiol. Biomarkers Prev.* **15**, 1159–1169 (2006).

45. McConnell, J. C. *et al.* Increased peri-ductal collagen micro-organization may contribute to raised mammographic density. *Breast Cancer Res.* **18**, 5 (2016).

46. Provenzano, P. P. *et al.* Collagen reorganization at the tumor-stromal interface facilitates local invasion. *BMC Med.* **4**, 38 (2006).

47. Conklin, M. W. *et al.* Aligned collagen is a prognostic signature for survival in human breast carcinoma. *Am. J. Pathol.* **178**, 1221–1232 (2011).

48. Xi, G. *et al.* Large-scale tumor-associated collagen signatures identify high-risk breast cancer patients. *Theranostics* **11**, 3229–3243 (2021).

49. Ray, A. *et al.* Stromal architecture directs early dissemination in pancreatic ductal adenocarcinoma. *JCI Insight* **7**, (2022).

50. Kirkpatrick, N. D., Brewer, M. A. & Utzinger, U. Endogenous optical biomarkers of ovarian cancer evaluated with multiphoton microscopy. *Cancer Epidemiol. Biomarkers Prev.* **16**, 2048–2057 (2007).

51. Wen, B. *et al.* 3D texture analysis for classification of second harmonic generation images of human ovarian cancer. *Sci. Rep.* **6**, 35734 (2016).

52. Sendín-Martín, M. *et al.* Quantitative collagen analysis using second harmonic generation images for the detection of basal cell carcinoma with ex vivo multiphoton microscopy. *Exp. Dermatol.* **32**, 392–402 (2023).

53. Laklai, H. *et al.* Genotype tunes pancreatic ductal adenocarcinoma tissue tension to induce matricellular fibrosis and tumor progression. *Nat. Med.* **22**, 497–505 (2016).

54. Almici, E. *et al.* Quantitative Image Analysis of Fibrillar Collagens Reveals Novel Diagnostic and Prognostic Biomarkers and Histotype-Dependent Aberrant Mechanobiology in Lung Cancer. *Mod. Pathol.* **36**, 100155 (2023).

55. Ikuta, D. *et al.* Fibrosis in metastatic lymph nodes is clinically correlated to poor prognosis in colorectal cancer. *Oncotarget* **9**, 29574–29586 (2018).

56. Pearce, O. M. T. *et al.* Deconstruction of a metastatic tumor microenvironment reveals a common matrix response in human cancers. *Cancer Discov.* **8**, 304–319 (2018).

57. Zhang, C. *et al.* Fibrotic microenvironment promotes the metastatic seeding of tumor cells via activating the fibronectin 1/secreted phosphoprotein 1-integrin signaling. *Oncotarget* **7**, 45702–45714 (2016).

58. Erler, J. T. *et al.* Hypoxia-induced lysyl oxidase is a critical mediator of bone marrow cell recruitment to form the premetastatic niche. *Cancer Cell* **15**, 35–44 (2009).

59. Cox, T. R. *et al.* LOX-mediated collagen crosslinking is responsible for fibrosis-enhanced metastasis. *Cancer Res.* **73**, 1721–1732 (2013).

60. Afasizheva, A. *et al.* Mitogen-activated protein kinase signaling causes malignant melanoma cells to differentially alter extracellular matrix biosynthesis to promote cell survival. *BMC Cancer* **16**, 186 (2016).

61. Farmer, P. *et al.* A stroma-related gene signature predicts resistance to neoadjuvant chemotherapy in breast cancer. *Nat. Med.* **15**, 68–74 (2009).

62. Principe, D. R. *et al.* Long-Term Gemcitabine Treatment Reshapes the Pancreatic Tumor Microenvironment and Sensitizes Murine Carcinoma to Combination Immunotherapy. *Cancer Res.* **80**, 3101–3115 (2020).

63. Shen, C. J. *et al.* Ionizing radiation induces tumor cell lysyl oxidase secretion. *BMC Cancer* **14**, 532 (2014).

64. Barker, H. E., Paget, J. T. E., Khan, A. A. & Harrington, K. J. The tumour microenvironment after radiotherapy: mechanisms of resistance and recurrence. *Nat. Rev. Cancer* **15**, 409–425 (2015).

65. Mancini, M. L. & Sonis, S. T. Mechanisms of cellular fibrosis associated with cancer regimen-related toxicities. *Front. Pharmacol.* **5**, 51 (2014).

66. Berestjuk, I. *et al.* Targeting Discoidin Domain Receptors DDR1 and DDR2 overcomes matrix-mediated tumor cell adaptation and tolerance to BRAF-targeted therapy in melanoma. *EMBO Mol. Med.* **14**, e11814 (2022).

67. Cuzick, J., Warwick, J., Pinney, E., Warren, R. M. L. & Duffy, S. W. Tamoxifen and breast density in women at increased risk of breast cancer. *J Natl Cancer Inst* **96**, 621–628 (2004).

68. Rhim, A. D. *et al.* Stromal elements act to restrain, rather than support, pancreatic ductal adenocarcinoma. *Cancer Cell* **25**, 735–747 (2014).

69. Maller, O. *et al.* Collagen architecture in pregnancy-induced protection from breast cancer. *J. Cell Sci.* **126**, 4108–4110 (2013).

70. Chandler, C., Liu, T., Buckanovich, R. & Coffman, L. G. The double edge sword of fibrosis in cancer. *Transl. Res.* **209**, 55–67 (2019).

71. Dibus, M., Joshi, O. & Ivaska, J. Novel tools to study cell-ECM interactions, cell adhesion dynamics and migration. *Curr. Opin. Cell Biol.* **88**, 102355 (2024).

72. Humphries, J. D., Byron, A. & Humphries, M. J. Integrin ligands at a glance. *J. Cell Sci.* **119**, 3901–3903 (2006).

73. Ray, A. & Provenzano, P. P. Aligned forces: Origins and mechanisms of cancer dissemination guided by extracellular matrix architecture. *Curr. Opin. Cell Biol.* **72**, 63–71 (2021).

74. Friedl, P. & Wolf, K. Plasticity of cell migration: a multiscale tuning model. *J. Cell Biol.* **188**, 11–19 (2010).

75. Hayen, W., Goebeler, M., Kumar, S., Riessen, R. & Nehls, V. Hyaluronan stimulates tumor cell migration by modulating the fibrin fiber architecture. *J. Cell Sci.* **112 (Pt 13)**, 2241–2251 (1999).

76. Murphy, C. M. & O'Brien, F. J. Understanding the effect of mean pore size on cell activity in collagen-glycosaminoglycan scaffolds. *Cell Adh. Migr.* **4**, 377–381 (2010).

77. Paul, C. D., Mistriotis, P. & Konstantopoulos, K. Cancer cell motility: lessons from migration in confined spaces. *Nat. Rev. Cancer* **17**, 131–140 (2017).

78. Short, B. Testing the limits of cell migration. *Journal of cell Biology* **201**, 965–965 (2013).

79. Wolf, K. *et al.* Physical limits of cell migration: control by ECM space and nuclear deformation and tuning by proteolysis and traction force. *J. Cell Biol.* **201**, 1069–1084 (2013).

80. Fischer, R. S. *et al.* Contractility, focal adhesion orientation, and stress fiber orientation drive cancer cell polarity and migration along wavy ECM substrates. *PNAS* **118**, e2021135118 (2021).

81. Zanotelli, M. R. *et al.* Regulation of ATP utilization during metastatic cell migration by collagen architecture. *Mol. Biol. Cell* **29**, 1–9 (2018).

82. Madamanchi, A., Zijlstra, A. & Zutter, M. M. Flipping the switch: integrin switching provides metastatic competence. *Sci. Signal.* **7**, pe9 (2014).

83. Samaržija, I. *et al.* Integrin crosstalk contributes to the complexity of signalling and unpredictable cancer cell fates. *Cancers (Basel)* **12**, (2020).

84. Di Martino, J. *et al.* The microenvironment controls invadosome plasticity. *J. Cell Sci.* **129**, 1759–1768 (2016).

85. Panková, K., Rösel, D., Novotný, M. & Brábek, J. The molecular mechanisms of transition between mesenchymal and amoeboid invasiveness in tumor cells. *Cell. Mol. Life Sci.* **67**, 63–71 (2010).

86. Haeger, A., Krause, M., Wolf, K. & Friedl, P. Cell jamming: collective invasion of mesenchymal tumor cells imposed by tissue confinement. *Biochim. Biophys. Acta* **1840**, 2386–2395 (2014).

87. Weigelin, B., Bakker, G.-J. & Friedl, P. Intravital third harmonic generation microscopy of collective melanoma cell invasion. *Intravital* **1**, 32–43 (2012).

88. Ilina, O. *et al.* Cell-cell adhesion and 3D matrix confinement determine jamming transitions in breast cancer invasion. *Nat. Cell Biol.* **22**, 1103–1115 (2020).

89. Khalil, A. A. *et al.* Collective invasion in ductal and lobular breast cancer associates with distant metastasis. *Clin. Exp. Metastasis* **34**, 421–429 (2017).

90. Provenzano, P. P. *et al.* Collagen density promotes mammary tumor initiation and progression. *BMC Med.* **6**, 11 (2008).

91. Gaggioli, C. *et al.* Fibroblast-led collective invasion of carcinoma cells with differing roles for RhoGTPases in leading and following cells. *Nat. Cell Biol.* **9**, 1392–1400 (2007).

92. Du, W., Xia, X., Hu, F. & Yu, J. Extracellular matrix remodeling in the tumor immunity. *Front. Immunol.* **14**, 1340634 (2023).

93. Yuan, Z. *et al.* Extracellular matrix remodeling in tumor progression and immune escape: from mechanisms to treatments. *Mol. Cancer* **22**, 48 (2023).

94. Kuczek, D. E. *et al.* Collagen density regulates the activity of tumor-infiltrating T cells. *J. Immunother. Cancer* **7**, 68 (2019).

95. Salmon, H. *et al.* Matrix architecture defines the preferential localization and migration of T cells into the stroma of human lung tumors. *J. Clin. Invest.* **122**, 899–910 (2012).

96. Byers, C. *et al.* Tertiary lymphoid structures accompanied by fibrillary matrix morphology impact anti-tumor immunity in basal cell carcinomas. *Front Med (Lausanne)* **9**, 981074 (2022).

97. Netti, P. A., Berk, D. A., Swartz, M. A., Grodzinsky, A. J. & Jain, R. K. Role of extracellular matrix assembly in interstitial transport in solid tumors. *Cancer Res.* **60**, 2497–2503 (2000).

98. Reyes-Ramos, A. M. *et al.* Collagen I Fibrous Substrates Modulate the Proliferation and Secretome of Estrogen Receptor-Positive Breast Tumor Cells in a Hormone-Restricted Microenvironment. *ACS Biomater. Sci. Eng.* **7**, 2430–2443 (2021).

99. Gomez, D., Natan, S., Shokef, Y. & Lesman, A. Mechanical Interaction between Cells Facilitates Molecular Transport. *Adv. Biosys.* **3**, e1900192 (2019).

100. Wijeratne, P. A., Hipwell, J. H., Hawkes, D. J., Stylianopoulos, T. & Vavourakis, V. Multiscale biphasic modelling of peritumoural collagen microstructure: The effect of tumour growth on permeability and fluid flow. *PLoS ONE* **12**, e0184511 (2017).

101. Jana, A., Ladner, K., Lou, E. & Nain, A. S. Tunneling Nanotubes between Cells Migrating in ECM Mimicking Fibrous Environments. *Cancers (Basel)* **14**, (2022).

102. Rustom, A., Saffrich, R., Markovic, I., Walther, P. & Gerdes, H.-H. Nanotubular highways for intercellular organelle transport. *Science* **303**, 1007–1010 (2004).

103. Mierke, C. T. Viscoelasticity, like forces, plays a role in mechanotransduction. *Front. Cell Dev. Biol.* **10**, 789841 (2022).

104. Chaudhuri, O., Cooper-White, J., Janmey, P. A., Mooney, D. J. & Shenoy, V. B. Effects of extracellular matrix viscoelasticity on cellular behaviour. *Nature* **584**, 535–546 (2020).

105. Wang, H., Abhilash, A. S., Chen, C. S., Wells, R. G. & Shenoy, V. B. Long-range force transmission in fibrous matrices enabled by tension-driven alignment of fibers. *Biophys. J.* **107**, 2592–2603 (2014).

106. Seo, B. R. *et al.* Collagen microarchitecture mechanically controls myofibroblast differentiation. *Proc Natl Acad Sci USA* **117**, 11387–11398 (2020).

107. Fattet, L. *et al.* Matrix Rigidity Controls Epithelial-Mesenchymal Plasticity and Tumor Metastasis via a Mechanoresponsive EPHA2/LYN Complex. *Dev. Cell* **54**, 302-316.e7 (2020).

108. Su, C.-Y. *et al.* Tumor stromal topography promotes chemoresistance in migrating breast cancer cell clusters. *Biomaterials* **298**, 122128 (2023).

109. Pradhan, S., Hassani, I., Clary, J. M. & Lipke, E. A. Polymeric biomaterials for in vitro cancer tissue engineering and drug testing applications. *Tissue Eng. Part B Rev.* **22**, 470–484 (2016).

110. Caliari, S. R. & Burdick, J. A. A practical guide to hydrogels for cell culture. *Nat. Methods* **13**, 405–414 (2016).

111. Unnikrishnan, K., Thomas, L. V. & Ram Kumar, R. M. Advancement of Scaffold-Based 3D Cellular Models in Cancer Tissue Engineering: An Update. *Front. Oncol.* **11**, 733652 (2021).

112. Passaniti, A., Kleinman, H. K. & Martin, G. R. Matrigel: history/background, uses, and future applications. *J. Cell Commun. Signal.* **16**, 621–626 (2022).

113. Sachs, N. *et al.* A living biobank of breast cancer organoids captures disease heterogeneity. *Cell* **172**, 373-386.e10 (2018).

114. Kaur, S., Kaur, I., Rawal, P., Tripathi, D. M. & Vasudevan, A. Non-matrigel scaffolds for organoid cultures. *Cancer Lett.* **504**, 58–66 (2021).

115. Curtis, K. J. *et al.* Mechanical stimuli and matrix properties modulate cancer spheroid growth in three-dimensional gelatin culture. *J. R. Soc. Interface* **17**, 20200568 (2020).

116. Linke, F. *et al.* 3D hydrogels reveal medulloblastoma subgroup differences and identify extracellular matrix subtypes that predict patient outcome. *J. Pathol.* **253**, 326–338 (2021).

117. Qiao, S.-P. *et al.* An alginate-based platform for cancer stem cell research. *Acta Biomater.* **37**, 83–92 (2016).

118. Vining, K. H., Stafford, A. & Mooney, D. J. Sequential modes of crosslinking tune viscoelasticity of cell-instructive hydrogels. *Biomaterials* **188**, 187–197 (2019).

119. Nam, S., Hu, K. H., Butte, M. J. & Chaudhuri, O. Strain-enhanced stress relaxation impacts nonlinear elasticity in collagen gels. *Proc Natl Acad Sci USA* **113**, 5492–5497 (2016).

120. Tse, J. R. & Engler, A. J. Preparation of hydrogel substrates with tunable mechanical properties. *Curr. Protoc. Cell Biol.* **Chapter 10**, Unit 10.16 (2010).

121. Levental, I., Georges, P. C. & Janmey, P. A. Soft biological materials and their impact on cell function. *Soft Matter* **3**, 299–306 (2007).

122. Ashworth, J. C. *et al.* Preparation of a User-Defined Peptide Gel for Controlled 3D Culture Models of Cancer and Disease. *J. Vis. Exp.* (2020) doi:10.3791/61710.

123. Gjorevski, N. & Lutolf, M. P. Synthesis and characterization of well-defined hydrogel matrices and their application to intestinal stem cell and organoid culture. *Nat. Protoc.* **12**, 2263–2274 (2017).

124. Richardson, T. *et al.* Engineered peptide modified hydrogel platform for propagation of human pluripotent stem cells. *Acta Biomater.* **113**, 228–239 (2020).

125. Rekad, Z., Izzi, V., Lamba, R., Ciais, D. & Van Obberghen-Schilling, E. The alternative matrisome: Alternative splicing of ECM proteins in development, homeostasis and tumor progression. *Matrix Biol.* **111**, 26–52 (2022).

126. Mredha, M. T. I. *et al.* A Facile Method to Fabricate Anisotropic Hydrogels with Perfectly Aligned Hierarchical Fibrous Structures. *Adv. Mater.* **30**, (2018).

127. Prince, E., Chen, Z., Khuu, N. & Kumacheva, E. Nanofibrillar hydrogel recapitulates changes occurring in the fibrotic extracellular matrix. *Biomacromolecules* **22**, 2352–2362 (2021).

128. Feng, C., Cheng, Y. & Chao, P. G. The influence and interactions of substrate thickness, organization and dimensionality on cell morphology and migration. *Acta Biomater.* **9**, 5502–5510 (2013).

129. Nerger, B. A., Brun, P. T. & Nelson, C. M. Marangoni flows drive the alignment of fibrillar cell-laden hydrogels. *Sci. Adv.* **6**, eaaz7748 (2020).

130. Mredha, M. T. I. *et al.* Anisotropic tough double network hydrogel from fish collagen and its spontaneous in vivo bonding to bone. *Biomaterials* **132**, 85–95 (2017).

131. Wallace, M., Cardoso, A. Z., Frith, W. J., Iggo, J. A. & Adams, D. J. Magnetically aligned supramolecular hydrogels. *Chem. Eur. J* **20**, 16484–16487 (2014).

132. Abalymov, A., Pinchasik, B.-E., Akasov, R. A., Lomova, M. & Parakhonskiy, B. V. Strategies for anisotropic fibrillar hydrogels: design, cell alignment, and applications in tissue engineering. *Biomacromolecules* **24**, 4532–4552 (2023).

133. Taufalele, P. V., VanderBurgh, J. A., Muñoz, A., Zanotelli, M. R. & Reinhart-King, C. A. Fiber alignment drives changes in architectural and mechanical features in collagen matrices. *PLoS ONE* **14**, e0216537 (2019).

134. Sapudom, J. *et al.* The phenotype of cancer cell invasion controlled by fibril diameter and pore size of 3D collagen networks. *Biomaterials* **52**, 367–375 (2015).

135. McCoy, M. G., Seo, B. R., Choi, S. & Fischbach, C. Collagen I hydrogel microstructure and composition conjointly regulate vascular network formation. *Acta Biomater.* **44**, 200–208 (2016).

136. Oh, S., Nguyen, Q. D., Chung, K.-H. & Lee, H. Bundling of collagen fibrils using sodium sulfate for biomimetic cell culturing. *ACS Omega* **5**, 3444–3452 (2020).

137. Riching, K. M. *et al.* 3D collagen alignment limits protrusions to enhance breast cancer cell persistence. *Biophys. J.* **107**, 2546–2558 (2014).

138. Su, C.-Y. *et al.* Engineering a 3D collective cancer invasion model with control over collagen fiber alignment. *Biomaterials* **275**, 120922 (2021).

139. Vader, D., Kabla, A., Weitz, D. & Mahadevan, L. Strain-induced alignment in collagen gels. *PLoS ONE* **4**, e5902 (2009).

140. Liu, C. *et al.* Self-assembly of mesoscale collagen architectures and applications in 3D cell migration. *Acta Biomater.* **155**, 167–181 (2023).

141. Gong, X., Kulwatno, J. & Mills, K. L. Rapid fabrication of collagen bundles mimicking tumor-associated collagen architectures. *Acta Biomater.* **108**, 128–141 (2020).

142. Dewavrin, J.-Y., Hamzavi, N., Shim, V. P. W. & Raghunath, M. Tuning the architecture of three-dimensional collagen hydrogels by physiological macromolecular crowding. *Acta Biomater.* **10**, 4351–4359 (2014).

143. Saiani, A. *et al.* Self-assembly and gelation properties of α-helix versus β-sheet forming peptides. *Soft Matter* **5**, 193–202 (2009).

144. Xie, J., Bao, M., Bruekers, S. M. C. & Huck, W. T. S. Collagen Gels with Different Fibrillar Microarchitectures Elicit Different Cellular Responses. *ACS Appl. Mater. Interfaces* **9**, 19630–19637 (2017).

145. Plou, J. *et al.* From individual to collective 3D cancer dissemination: roles of collagen concentration and TGF-β. *Sci. Rep.* **8**, 12723 (2018).

146. Berger, A. J., Linsmeier, K. M., Kreeger, P. K. & Masters, K. S. Decoupling the effects of stiffness and fiber density on cellular behaviors via an interpenetrating network of gelatin-methacrylate and collagen. *Biomaterials* **141**, 125–135 (2017).

147. Velez, D. O. *et al.* 3D collagen architecture induces a conserved migratory and transcriptional response linked to vasculogenic mimicry. *Nat. Commun.* **8**, 1651 (2017).

148. Ranamukhaarachchi, S. K. *et al.* Macromolecular crowding tunes 3D collagen architecture and cell morphogenesis. *Biomater. Sci.* **7**, 618–633 (2019).

149. Cavo, M. *et al.* Electrospun nanofibers in cancer research: from engineering of in vitro 3D cancer models to therapy. *Biomater. Sci.* **8**, 4887–4905 (2020).

150. Fong, E. L. S. *et al.* Modeling Ewing sarcoma tumors in vitro with 3D scaffolds. *Proc Natl Acad Sci USA* **110**, 6500–6505 (2013).

151. Ameer, J. M., Pr, A. K. & Kasoju, N. Strategies to tune electrospun scaffold porosity for effective cell response in tissue engineering. *J. Funct. Biomater.* **10**, (2019).

152. Saha, S. *et al.* Electrospun fibrous scaffolds promote breast cancer cell alignment and epithelial-mesenchymal transition. *Langmuir* **28**, 2028–2034 (2012).

153. Wang, K. *et al.* Creation of macropores in electrospun silk fibroin scaffolds using sacrificial PEO-microparticles to enhance cellular infiltration. *J. Biomed. Mater. Res. A* **101**, 3474–3481 (2013).

154. Yucheng, Y., Glubay, S., Stirling, R., Ma, Q. & McKenzie, J. Improved fiber control through ohmic/convective flow behavior. *J. Mater. Sci.* **57**, 10457–10469 (2022).

155. Wang, M. *et al.* Regulating Mechanotransduction in Three Dimensions using Sub-Cellular Scale, Crosslinkable Fibers of Controlled Diameter, Stiffness, and Alignment. *Adv. Funct. Mater.* **29**, (2019).

156. Hoogenkamp, H. R. *et al.* Directing collagen fibers using counter-rotating cone extrusion. *Acta Biomater.* **12**, 113–121 (2015).

157. Yang, S. *et al.* Oriented collagen fiber membranes formed through counter-rotating extrusion and their application in tendon regeneration. *Biomaterials* **207**, 61–75 (2019).

158. Hong, J., Yeo, M., Yang, G. H. & Kim, G. Cell-Electrospinning and Its Application for Tissue Engineering. *Int. J. Mol. Sci.* **20**, (2019).

159. Grossman, M. *et al.* Tumor cell invasion can be blocked by modulators of collagen fibril alignment that control assembly of the extracellular matrix. *Cancer Res.* **76**, 4249–4258 (2016).

160. Visser, D. *et al.* Electrospinning of collagen: enzymatic and spectroscopic analyses reveal solvent-independent disruption of the triple-helical structure. *J. Mater. Chem. B Mater. Biol. Med.* **11**, 2207–2218 (2023).

161. Prieto, E. I., Mojares, E. B. A., Cortez, J. J. M. & Vasquez, M. R. Electrospun nanofiber scaffolds for the propagation and analysis of breast cancer stem cells in vitro. *Biomed. Mater.* **16**, 035004 (2021).

162. Zeugolis, D. I. *et al.* Electro-spinning of pure collagen nano-fibres - just an expensive way to make gelatin? *Biomaterials* **29**, 2293–2305 (2008).

163. Jordahl, S. *et al.* Engineered Fibrillar Fibronectin Networks as Three-Dimensional Tissue Scaffolds. *Adv. Mater.* **31**, e1904580 (2019).

164. Hiraki, H. L. *et al.* Magnetic alignment of electrospun fiber segments within a hydrogel composite guides cell spreading and migration phenotype switching. *Front. Bioeng. Biotechnol.* **9**, 679165 (2021).

165. Sundararaghavan, H. G., Saunders, R. L., Hammer, D. A. & Burdick, J. A. Fiber alignment directs cell motility over chemotactic gradients. *Biotechnol. Bioeng.* **110**, 1249–1254 (2013).

166. Yang, F., Han, L.-H. & Tong, X. Dynamic Macropore Formation Using Multiple Porogens. (2014).

167. Ricci, C. *et al.* Interfacing polymeric scaffolds with primary pancreatic ductal adenocarcinoma cells to develop 3D cancer models. *Biomatter* **4**, e955386 (2014).

168. Du, L. *et al.* Hierarchical macro/micro-porous silk fibroin scaffolds for tissue engineering. *Mater. Lett.* **236**, 1–4 (2019).

169. Tammaro, D., Villone, M. M., D'Avino, G. & Maffettone, P. L. An experimental and numerical investigation on bubble growth in polymeric foams. *Entropy (Basel)* **24**, (2022).

170. Chen, G., Ushida, T. & Tateishi, T. Scaffold Design for Tissue Engineering. *Macromol. Biosci.* **2**, 67–77 (2002).

171. Loh, Q. L. & Choong, C. Three-dimensional scaffolds for tissue engineering applications: role of porosity and pore size. *Tissue Eng. Part B Rev.* **19**, 485–502 (2013).

172. Annabi, N. *et al.* Controlling the porosity and microarchitecture of hydrogels for tissue engineering. *Tissue Eng. Part B Rev.* **16**, 371–383 (2010).

173. Ma, P. X. Scaffolds for tissue fabrication. *Materials Today* **7**, 30–40 (2004).

174. Lin, A. S. P., Barrows, T. H., Cartmell, S. H. & Guldberg, R. E. Microarchitectural and mechanical characterization of oriented porous polymer scaffolds. *Biomaterials* **24**, 481–489 (2003).

175. Woo, K. M., Chen, V. J. & Ma, P. X. Nano-fibrous scaffolding architecture selectively enhances protein adsorption contributing to cell attachment. *J. Biomed. Mater. Res. A* **67**, 531–537 (2003).

176. Aguado, B. A. *et al.* Extracellular matrix mediators of metastatic cell colonization characterized using scaffold mimics of the pre-metastatic niche. *Acta Biomater.* **33**, 13–24 (2016).

177. Schoof, H., Apel, J., Heschel, I. & Rau, G. Control of pore structure and size in freeze-dried collagen sponges. *J. Biomed. Mater. Res.* **58**, 352–357 (2001).

178. Schoof, H., Bruns, L., Fischer, A., Heschel, I. & Rau, G. Dendritic ice morphology in unidirectionally solidified collagen suspensions. *J. Cryst. Growth* **209**, 122–129 (2000).

179. Kang, H. W., Tabata, Y. & Ikada, Y. Fabrication of porous gelatin scaffolds for tissue engineering. *Biomaterials* **20**, 1339–1344 (1999).

180. Davidenko, N. *et al.* Biomimetic collagen scaffolds with anisotropic pore architecture. *Acta Biomater.* **8**, 667–676 (2012).

181. Faraj, K. A., van Kuppevelt, T. H. & Daamen, W. F. Construction of collagen scaffolds that mimic the three-dimensional architecture of specific tissues. *Tissue Eng.* **13**, 2387–2394 (2007).

182. Shepherd, J. H. *et al.* Structurally graduated collagen scaffolds applied to the ex vivo generation of platelets from human pluripotent stem cell-derived megakaryocytes: Enhancing production and purity. *Biomaterials* **182**, 135–144 (2018).

183. Campbell, J. J., Husmann, A., Hume, R. D., Watson, C. J. & Cameron, R. E. Development of three-dimensional collagen scaffolds with controlled architecture for cell migration studies using breast cancer cell lines. *Biomaterials* **114**, 34–43 (2017).

184. Hume, R. D. *et al.* Tumour cell invasiveness and response to chemotherapeutics in adipocyte invested 3D engineered anisotropic collagen scaffolds. *Sci. Rep.* **8**, 12658 (2018).

185. Yannas, I. V., Lee, E., Orgill, D. P., Skrabut, E. M. & Murphy, G. F. Synthesis and characterization of a model extracellular matrix that induces partial regeneration of adult mammalian skin. *Proc Natl Acad Sci USA* **86**, 933–937 (1989).

186. Hofmann, S. *et al.* Control of in vitro tissue-engineered bone-like structures using human mesenchymal stem cells and porous silk scaffolds. *Biomaterials* **28**, 1152–1162 (2007).

187. Lu, H., Ko, Y.-G., Kawazoe, N. & Chen, G. Cartilage tissue engineering using funnel-like collagen sponges prepared with embossing ice particulate templates. *Biomaterials* **31**, 5825–5835 (2010).

188. Wolf, K. *et al.* Collagen-based cell migration models in vitro and in vivo. *Semin. Cell Dev. Biol.* **20**, 931–941 (2009).

189. Cyr, J. A., Husmann, A., Best, S. M. & Cameron, R. E. Complex architectural control of ice-templated collagen scaffolds using a predictive model. *Acta Biomater.* **153**, 260–272 (2022).

190. Pawelec, K. M., Husmann, A., Best, S. M. & Cameron, R. E. A design protocol for tailoring ice-templated scaffold structure. *J. R. Soc. Interface* **11**, 20130958 (2014).

191. Song, X., Philpott, M. A., Best, S. M. & Cameron, R. E. Controlling the Architecture of Freeze-Dried Collagen Scaffolds with Ultrasound-Induced Nucleation. *Polymers (Basel)* **16**, (2024).

192. Buttafoco, L. *et al.* First steps towards tissue engineering of small-diameter blood vessels: preparation of flat scaffolds of collagen and elastin by means of freeze drying. *J. Biomed. Mater. Res. Part B Appl. Biomater.* **77**, 357–368 (2006).

193. Yang, F. *et al.* Manufacturing and morphology structure of polylactide-type microtubules orientation-structured scaffolds. *Biomaterials* **27**, 4923–4933 (2006).

194. Ashworth, J. C., Mehr, M., Buxton, P. G., Best, S. M. & Cameron, R. E. Cell invasion in collagen scaffold architectures characterized by percolation theory. *Adv. Healthc. Mater.* **4**, 1317–1321 (2015).

195. Caliari, S. R. *et al.* Collagen scaffold arrays for combinatorial screening of biophysical and biochemical regulators of cell behavior. *Adv. Healthc. Mater.* **4**, 58–64 (2015).

196. Mayorca-Guiliani, A. E. *et al.* ISDoT: in situ decellularization of tissues for high-resolution imaging and proteomic analysis of native extracellular matrix. *Nat. Med.* **23**, 890–898 (2017).

197. Jamaluddin, M. F. B. *et al.* Bovine and human endometrium-derived hydrogels support organoid culture from healthy and cancerous tissues. *Proc Natl Acad Sci USA* **119**, e2208040119 (2022).

198. Sensi, F. *et al.* Establishment of a human 3D pancreatic adenocarcinoma model based on a patient-derived extracellular matrix scaffold. *Transl. Res.* **253**, 57–67 (2023).

199. Tian, X. *et al.* Organ-specific metastases obtained by culturing colorectal cancer cells on tissue-specific decellularized scaffolds. *Nat. Biomed. Eng.* **2**, 443–452 (2018).

200. Fitzpatrick, L. E. & McDevitt, T. C. Cell-derived matrices for tissue engineering and regenerative medicine applications. *Biomater. Sci.* **3**, 12–24 (2015).

201. Ragelle, H. *et al.* Comprehensive proteomic characterization of stem cell-derived extracellular matrices. *Biomaterials* **128**, 147–159 (2017).

202. Rubí-Sans, G. *et al.* Development of Cell-Derived Matrices for Three-Dimensional In Vitro Cancer Cell Models. *ACS Appl. Mater. Interfaces* **13**, 44108–44123 (2021).

203. Almici, E., Caballero, D., Montero Boronat, J. & Samitier Martí, J. Engineering cell-derived matrices with controlled 3D architectures for pathophysiological studies. *Methods Cell Biol.* **156**, 161–183 (2020).

204. Saldin, L. T., Cramer, M. C., Velankar, S. S., White, L. J. & Badylak, S. F. Extracellular matrix hydrogels from decellularized tissues: Structure and function. *Acta Biomater.* **49**, 1–15 (2017).

205. Caballero, D. & Samitier, J. Topological Control of Extracellular Matrix Growth: A Native-Like Model for Cell Morphodynamics Studies. *ACS Appl. Mater. Interfaces* **9**, 4159–4170 (2017).

206. Caballero, D., Palacios, L., Freitas, P. P. & Samitier, J. An Interplay between Matrix Anisotropy and Actomyosin Contractility Regulates 3D-Directed Cell Migration. *Adv. Funct. Mater.* **27**, (2017).

207. Casale, C., Imparato, G., Mazio, C., Netti, P. A. & Urciuolo, F. Geometrical confinement controls cell, ECM and vascular network alignment during the morphogenesis of 3D bioengineered human connective tissues. *Acta Biomater.* **131**, 341–354 (2021).

208. Wilks, B. T. *et al.* Quantifying Cell-Derived Changes in Collagen Synthesis, Alignment, and Mechanics in a 3D Connective Tissue Model. *Adv Sci (Weinh)* **9**, e2103939 (2022).

209. Huang, G. *et al.* Functional and Biomimetic Materials for Engineering of the Three-Dimensional Cell Microenvironment. *Chem. Rev.* **117**, 12764–12850 (2017).

210. Franco-Barraza, J., Beacham, D. A., Amatangelo, M. D. & Cukierman, E. Preparation of extracellular matrices produced by cultured and primary fibroblasts. *Curr. Protoc. Cell Biol.* **71**, 10.9.1-10.9.34 (2016).

211. Murphy, K. J. *et al.* Cell-derived Matrix Assays to Assess Extracellular Matrix Architecture and Track Cell Movement. *Bio Protoc* **12**, (2022).

212. Chan, W. W. *et al.* Towards Biomanufacturing of Cell-Derived Matrices. *Int. J. Mol. Sci.* **22**, (2021).

213. Jones, S. *et al.* Application of a 3D hydrogel-based model to replace use of animals for passaging patient-derived xenografts. *In vitro models* **2**, 99–111 (2023).

214. Conway, J. R. W. *et al.* Three-dimensional organotypic matrices from alternative collagen sources as pre-clinical models for cell biology. *Sci. Rep.* **7**, 16887 (2017).

215. Ye, Z., Wandall, H. H. & Dabelsteen, S. Phosphoproteomic analysis and organotypic cultures for the study of signaling pathways. *Bio Protoc* **14**, e4941 (2024).

216. Baker, B. M. *et al.* Cell-mediated fibre recruitment drives extracellular matrix mechanosensing in engineered fibrillar microenvironments. *Nat. Mater.* **14**, 1262–1268 (2015).

217. Lim, K. S. *et al.* Fundamentals and Applications of Photo-Cross-Linking in Bioprinting. *Chem. Rev.* **120**, 10662–10694 (2020).

218. ISO/ASTM International. ISO/ASTM 52900: Additive manufacturing — General principles — Fundamentals and vocabulary. **Second edition**, (2021).

219. Shapira, A. & Dvir, T. 3D Tissue and Organ Printing-Hope and Reality. *Adv Sci (Weinh)* **8**, 2003751 (2021).

220. Spagnolo, B. *et al.* Three-dimensional cage-like microscaffolds for cell invasion studies. *Sci. Rep.* **5**, 10531 (2015).

221. Tayalia, P., Mendonca, C. R., Baldacchini, T., Mooney, D. J. & Mazur, E. 3D Cell-Migration Studies using Two-Photon Engineered Polymer Scaffolds. *Adv. Mater.* **20**, 4494–4498 (2008).

222. Alkmin, S. *et al.* Migration dynamics of ovarian epithelial cells on micro-fabricated image-based models of normal and malignant stroma. *Acta Biomater.* **100**, 92–104 (2019).

223. Zandrini, T., Florczak, S., Levato, R. & Ovsianikov, A. Breaking the resolution limits of 3D bioprinting: future opportunities and present challenges. *Trends Biotechnol.* **41**, 604–614 (2023).

224. Castilho, M. *et al.* Hydrogel-Based Bioinks for Cell Electrowriting of Well-Organized Living Structures with Micrometer-Scale Resolution. *Biomacromolecules* **22**, 855–866 (2021).

225. Zandrini, T. *et al.* Multi-foci laser microfabrication of 3D polymeric scaffolds for stem cell expansion in regenerative medicine. *Sci. Rep.* **9**, 11761 (2019).

226. Atry, F. *et al.* Parallel multiphoton excited fabrication of tissue engineering scaffolds using a diffractive optical element. *Opt. Express* **28**, 2744–2757 (2020).

227. Ouyang, W. *et al.* Ultrafast 3D nanofabrication via digital holography. *Nat. Commun.* **14**, 1716 (2023).

228. Saha, S. K. *et al.* Scalable submicrometer additive manufacturing. *Science* **366**, 105–109 (2019).

229. Dobos, A. *et al.* Thiol-Gelatin-Norbornene Bioink for Laser-Based High-Definition Bioprinting. *Adv. Healthc. Mater.* **9**, e1900752 (2020).

230. Puiggalí-Jou, A. *et al.* FLight Biofabrication Supports Maturation of Articular Cartilage with Anisotropic Properties. *Adv. Healthc. Mater.* e2302179 (2023) doi:10.1002/adhm.202302179.

231. Liu, H. *et al.* Filamented Light (FLight) Biofabrication of Highly Aligned Tissue-Engineered Constructs. *Adv. Mater.* **34**, e2204301 (2022).

232. Nerger, B. A., Brun, P. T. & Nelson, C. M. Microextrusion printing cell-laden networks of type I collagen with patterned fiber alignment and geometry. *Soft Matter* **15**, 5728–5738 (2019).

233. Huang, Y., Agrawal, B., Sun, D., Kuo, J. S. & Williams, J. C. Microfluidics-based devices: New tools for studying cancer and cancer stem cell migration. *Biomicrofluidics* **5**, 13412 (2011).

234. Sontheimer-Phelps, A., Hassell, B. A. & Ingber, D. E. Modelling cancer in microfluidic human organs-on-chips. *Nat. Rev. Cancer* **19**, 65–81 (2019).

235. Davidson, P. M., Sliz, J., Isermann, P., Denais, C. & Lammerding, J. Design of a microfluidic device to quantify dynamic intra-nuclear deformation during cell migration through confining environments. *Integr Biol (Camb)* **7**, 1534–1546 (2015).

236. Lee, P., Lin, R., Moon, J. & Lee, L. P. Microfluidic alignment of collagen fibers for in vitro cell culture. *Biomed. Microdevices* **8**, 35–41 (2006).

237. Drifka, C. R. *et al.* Comparison of picrosirius red staining with second harmonic generation imaging for the quantification of clinically relevant collagen fiber features in histopathology samples. *J. Histochem. Cytochem.* **64**, 519–529 (2016).

238. Marcos-Garcés, V., Harvat, M., Molina Aguilar, P., Ferrández Izquierdo, A. & Ruiz-Saurí, A. Comparative measurement of collagen bundle orientation by Fourier analysis and semiquantitative evaluation: reliability and agreement in Masson's trichrome, Picrosirius red and confocal microscopy techniques. *J. Microsc.* **267**, 130–142 (2017).

239. Abd-Elgaliel, W. R. & Tung, C.-H. Exploring the structural requirements of collagen-binding peptides. *Biopolymers* **100**, 167–173 (2013).

240. Haddad, T. S. *et al.* Tutorial: methods for three-dimensional visualization of archival tissue material. *Nat. Protoc.* **16**, 4945–4962 (2021).

241. Yu, T., Zhu, J., Li, D. & Zhu, D. Physical and chemical mechanisms of tissue optical clearing. *iScience* **24**, 102178 (2021).

242. Vielreicher, M. *et al.* Taking a deep look: modern microscopy technologies to optimize the design and functionality of biocompatible scaffolds for tissue engineering in regenerative medicine. *J. R. Soc. Interface* **10**, 20130263 (2013).

243. Katsamenis, O. L. *et al.* X-ray Micro-Computed Tomography for Nondestructive Three-Dimensional (3D) X-ray Histology. *Am. J. Pathol.* **189**, 1608–1620 (2019).

244. Ouni, E. *et al.* A blueprint of the topology and mechanics of the human ovary for next-generation bioengineering and diagnosis. *Nat. Commun.* **12**, 5603 (2021).

245. Bushby, A. J. *et al.* Imaging three-dimensional tissue architectures by focused ion beam scanning electron microscopy. *Nat. Protoc.* **6**, 845–858 (2011).

246. Cicchi, R. *et al.* From molecular structure to tissue architecture: collagen organization probed by SHG microscopy. *J. Biophotonics* **6**, 129–142 (2013).

247. Keikhosravi, A. *et al.* Quantification of collagen organization in histopathology samples using liquid crystal based polarization microscopy. *Biomed. Opt. Express* **8**, 4243–4256 (2017).

248. Freudiger, C. W. *et al.* Label-free biomedical imaging with high sensitivity by stimulated Raman scattering microscopy. *Science* **322**, 1857–1861 (2008).

249. Becker, L. *et al.* Raman microspectroscopy identifies fibrotic tissues in collagen-related disorders via deconvoluted collagen type I spectra. *Acta Biomater.* **162**, 278–291 (2023).

250. Butler, H. J. *et al.* Using Raman spectroscopy to characterize biological materials. *Nat. Protoc.* **11**, 664–687 (2016).

251. Kreiss, L. *et al.* Label-free analysis of inflammatory tissue remodeling in murine lung tissue based on multiphoton microscopy, Raman spectroscopy and machine learning. *J. Biophotonics* **15**, e202200073 (2022).

252. Eekhoff, J. D. & Lake, S. P. Three-dimensional computation of fibre orientation, diameter and branching in segmented image stacks of fibrous networks. *J. R. Soc. Interface* **17**, 20200371 (2020).

253. Liu, Z. *et al.* Rapid three-dimensional quantification of voxel-wise collagen fiber orientation. *Biomed. Opt. Express* **6**, 2294–2310 (2015).

254. Wershof, E. *et al.* A FIJI macro for quantifying pattern in extracellular matrix. *Life Sci. Alliance* **4**, (2021).

255. Devlin, M.-J. *et al.* The Tumor Microenvironment of Clear-Cell Ovarian Cancer. *Cancer Immunol. Res.* **10**, 1326–1339 (2022).

256. Liu, Y. *et al.* Fibrillar collagen quantification with curvelet transform based computational methods. *Front. Bioeng. Biotechnol.* **8**, 198 (2020).

257. Sorelli, M. *et al.* Fiber enhancement and 3D orientation analysis in label-free two-photon fluorescence microscopy. *Sci. Rep.* **13**, 4160 (2023).

258. Bumgarner, J. R. & Nelson, R. J. Open-source analysis and visualization of segmented vasculature datasets with VesselVio. *Cell Rep. Methods* **2**, 100189 (2022).

259. Spangenberg, P. *et al.* Rapid and fully automated blood vasculature analysis in 3D light-sheet image volumes of different organs. *Cell Rep. Methods* **3**, 100436 (2023).

260. Sapudom, J. *et al.* Collagen fibril orientation instructs fibroblast differentiation via cell contractility. *Adv Sci (Weinh)* **10**, e2301353 (2023).

261. Joukhdar, H. *et al.* Imparting Multi-Scalar Architectural Control into Silk Materials Using a Simple Multi-Functional Ice-Templating Fabrication Platform. *Adv. Mater. Technol.* 2201642 (2023) doi:10.1002/admt.202201642.

262. Joshi, I. M. *et al.* Microengineering 3D Collagen Matrices with Tumor-Mimetic Gradients in Fiber Alignment. *Adv. Funct. Mater.* (2023) doi:10.1002/adfm.202308071.

263. Osuna de la Peña, D. *et al.* Bioengineered 3D models of human pancreatic cancer recapitulate in vivo tumour biology. *Nat. Commun.* **12**, 5623 (2021).

264. Vega, S. L. *et al.* Combinatorial hydrogels with biochemical gradients for screening 3D cellular microenvironments. *Nat. Commun.* **9**, 614 (2018).

265. Yang, Y., Motte, S. & Kaufman, L. J. Pore size variable type I collagen gels and their interaction with glioma cells. *Biomaterials* **31**, 5678–5688 (2010).

266. Cavo, M. *et al.* Microenvironment complexity and matrix stiffness regulate breast cancer cell activity in a 3D in vitro model. *Sci. Rep.* **6**, 35367 (2016).